

InstructMix2Mix: Consistent Sparse-View Editing Through Multi-View Model Personalization

Daniel Gilo¹ Or Litany^{1,2}

¹Technion – Israel Institute of Technology

²NVIDIA

danielgilo@cs.technion.ac.il or.litany@gmail.com

Abstract

We address the task of multi-view image editing from sparse input views, where the inputs can be seen as a mix of images capturing the scene from different viewpoints. The goal is to modify the scene according to a textual instruction while preserving consistency across all views. Existing methods, based on per-scene neural fields or temporal attention mechanisms, struggle in this setting, often producing artifacts and incoherent edits. We propose *Instruct-Mix2Mix (I-Mix2Mix)*, a framework that distills the editing capabilities of a 2D diffusion model into a pretrained multi-view diffusion model, leveraging its data-driven 3D prior for cross-view consistency. A key contribution is replacing the conventional neural field consolidator in *Score Distillation Sampling (SDS)* with a multi-view diffusion student, which requires novel adaptations: incremental student updates across timesteps, a specialized teacher noise scheduler to prevent degeneration, and an attention modification that enhances cross-view coherence without additional cost. Experiments demonstrate that *I-Mix2Mix* significantly improves multi-view consistency while maintaining high per-frame edit quality. Additional visualizations and code are available on our [project page](#).

1. Introduction

Multi-view image editing seeks to modify a scene captured from multiple viewpoints while preserving consistency across views. Typical edits include texture and color changes, semantic manipulations, or geometric transformations, with applications in product imagery, real-estate and interior design visualization, AR/VR, and cinematic post-production.

However, multi-view editing is a difficult task that traditionally requires skilled artists, making automation highly desirable. In recent years, a variety of methods have been proposed for editing 3D scenes. Due to the difficulty of pro-

ducing supervision in the form of high-quality paired scenes before and after editing, most of these approaches avoid direct multi-view editing, instead leveraging monocular editors such as *InstructPix2Pix* [7], either iteratively [22, 61] or through distillation [31, 39]. These approaches achieve 3D-consistent edits by operating on dense scene representations like NeRFs [46] or 3D Gaussian Splats [32]. However, in many real-world scenarios, users have access only to a sparse set of views—such as a few casually captured photos or product images—which provide limited scene coverage and challenge existing 3D editing methods to maintain geometric and appearance consistency.

In this work, we tackle the challenging problem of multi-view editing from sparse input images (a *mix* of images). Given a few source views and a textual editing instruction, our aim is to generate edits that faithfully follow the prompt while remaining consistent across all viewpoints. Following prior work, we leverage powerful 2D editors and lift their capabilities to 3D using *Score Distillation Sampling (SDS)* [50]. However, we propose a new approach to this paradigm. We observe that current approaches face inherent limitations. Neural field representations are trained per scene – they do not hold 3D prior in their network weights. Instead, they achieve 3D consistency by incorporating a physical prior through the rendering equations. A *dense set* of input images is required, however, to transform this prior into an effective consolidator. To achieve consistency with *sparse* views, we instead propose to incorporate a consolidator that embeds a strong, data-driven 3D prior directly in its weights: a multi-view synthesis diffusion model. While such models are trained to generate view-consistent scenes (e.g., from text or images), they lack editing capabilities. We bridge this gap by combining the strengths of both paradigms—distilling edits from a 2D editor (the teacher) into the multi-view model (the student). Concretely, we use *InstructPix2Pix* as the teacher and *Stable Virtual Camera (SEVA)* [76] as the student. By leveraging a student model with an inherent 3D prior, our method — **I-Mix2Mix** —

produces robust, geometrically coherent, and visually consistent edits even from extremely sparse inputs.

Replacing the neural field with a multi-view diffusion model within the SDS framework is not straightforward, and requires careful adaptation of several key steps. Instead of rendering from a scene representation, we sample from the diffusion model; to avoid costly full trajectories, we distill incrementally across student timesteps. We also introduce a specialized teacher noise scheduler to prevent collapse to poor local minima and an attention modification that strengthens multi-view consistency without extra cost. Together, these components yield a framework for consistent multi-view editing, producing high-quality results even with very sparse inputs.

To summarize, our contributions are:

1. We present I-Mix2Mix, a novel framework for distilling the knowledge of a powerful monocular editor into a pretrained multi-view diffusion model, leveraging its data-driven 3D consistency.
2. Through careful consideration of the SDS key steps, we introduce novel adaptations to support personalization of our multi-view student.
3. We demonstrate that this approach produces high-quality, consistent multi-view edits, effectively extending the SDS framework to scenarios with limited viewpoints.

We evaluate I-Mix2Mix against popular multi-view editing methods, demonstrating significant improvements in cross-view consistency both qualitatively and quantitatively in the sparse-view setting. At the same time, our method maintains competitive per-frame editing performance, highlighting the practical benefits of leveraging a data-driven multi-view prior within the SDS framework.

2. Related Works

3D editing. Editing 3D scenes or objects typically assumes a pre-optimized model such as a NeRF [46] or 3DGS [32]. Early works explored *direct NeRF manipulation* via scribbles [40], sketches [45], reference images [4], meshes [72], point clouds [10], and other cues [47, 68, 71], while *NeRF stylization* transfers reference appearances to 3D scenes [15, 28, 48, 64, 65]. *Instruction-based* approaches leverage 2D diffusion editors like InstructPix2Pix [7], applying SDS-like guidance [27, 31, 39, 55, 79] or Iterative Dataset Update [9, 13, 22, 61, 63, 66] for improved consistency. Some methods [17, 21, 37] further enforce alignment using depth information from the trained NeRF, while others [11, 49, 70] operate directly in a learned 3D latent space. While effective for 3D editing, the reliance of these approaches on dense input views or an initial 3D representation makes them less suitable in sparse-view scenarios.

Sparse multi-view editing. In the absence of a full 3D representation, several works have explored editing a set of input images directly. A prominent direction adapts pre-trained diffusion-based monocular editors by modifying self-attention layers: as first shown in Wu et al. [69], extending queries to attend across frames promotes consistency between the outputs. Building on this idea, a number of methods generate edited image sequences [8, 20, 33, 41, 51, 56, 78]. While effective for temporally smooth sequences with small viewpoint changes, these approaches struggle in the sparse-view setting, where edits must remain consistent under significant viewpoint differences. DGE [12] combines extended attention with 3D Gaussian Splatting (3DGS) lifting: attention-based edits provide rough multi-view consistency, while 3DGS is used to consolidate outputs and resolve residual artifacts. However, in the sparse-view regime, 3DGS tends to overfit the limited input views rather than serve as a true cross-view aggregator [73, 77], leading to persistent inconsistencies. As a result, DGE effectively reduces to an extended-attention approach, inheriting the same limitations as prior video editing methods. Most recently, Bar-On et al. [5] proposed a feed-forward approach that propagates a user-provided 2D edit to multiple views, but their method remains limited to object-level edits. Contemporaneously with our work, Zhao et al. [75] fine-tune FLUX Kontext [35] to enable consistent edits across image pairs, while [14, 60] distill 3D consistency priors into a 2D editor.

3. Preliminaries

Stable Virtual Camera. SEVA [76] is a diffusion-based Novel View Synthesis (NVS) model that predicts N target images given M input images with their camera poses. Built on Stable Diffusion 2.1 [54] with architectural adaptations for NVS and trained on diverse object and scene datasets, it achieves state-of-the-art results, making it an ideal student model with a strong 3D prior.

Instruct-Pix2Pix. A monocular, instruction-based image editing diffusion model widely used in 3D and multi-view editing, Instruct-Pix2Pix [7] is fine-tuned from a pre-trained Stable Diffusion model on a large-scale synthetic editing dataset. Given a source image and a textual instruction, it produces versatile edits by sampling the fine-tuned model. The model employs classifier-free guidance (CFG) [23] with two scales: a *text CFG scale* s_T controlling adherence to the instruction, and an *image CFG scale* s_I controlling fidelity to the source image, jointly balancing edit strength and overall image quality.

4. Method

Our goal is sparse multi-view consistent image editing. We build on the SDS framework [50], using a pre-trained im-

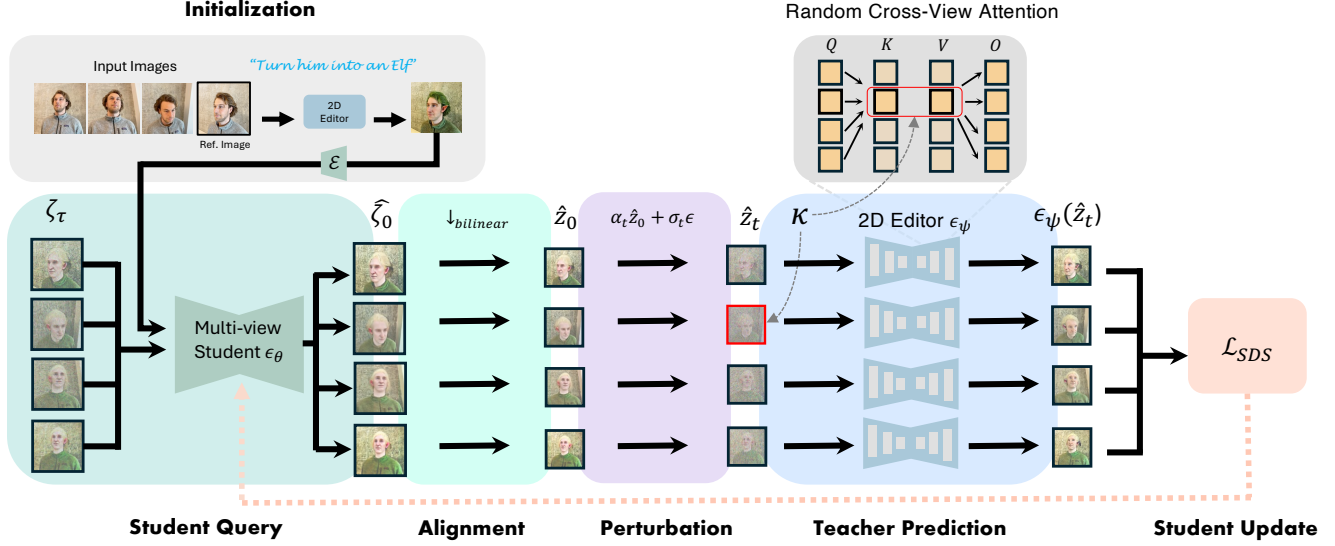


Figure 1. **I-Mix2Mix overview.** Given a set of input images, a randomly chosen reference image is edited by the frozen teacher and encoded to serve as the personalized multi-view student’s input latent (*Initialization*). At each distillation iteration, noisy multi-view latents ζ_τ are denoised by the student (*Student Query*), aligned to the teacher’s latent space (*Alignment*), and perturbed with our forward schedule (*Perturbation*). The teacher predicts edits with Random Cross-View Attention (*Teacher Prediction*), where all frames attend to the κ ’s frame, and the resulting supervision is distilled back into the student (*Student Update*). After distillation, the student outputs a set of multi-view consistent edited frames.

age editing network as a *teacher* to distill knowledge into a neural scene representation *student*. Unlike typical settings that assume abundant input views, we work with only a few images. To address this challenge, we replace the conventional neural field with a multi-view diffusion model pre-trained for consistent view generation. We personalize this student to the target scene and edit instruction by distilling the teacher’s predictions, enabling faithful and consistent edits from limited inputs.

4.1. Problem Formulation

We are given N images $\{I_i\}_{i=1}^N$, $I_i \in \mathbb{R}^{3 \times H \times W}$ of a static 3D scene with camera poses $\{\pi_i\}_{i=1}^N$, $\pi_i \in \mathbb{R}^{4 \times 4}$, and an editing prompt $y \in \mathcal{Y}$. We assume access to a multi-view diffusion model ϵ_θ which we refer to as the *student*, and a monocular instruction-based editing diffusion model (*teacher*) ϵ_ψ . The goal is to produce edited views $\{E_i\}_{i=1}^N$ such that (i) each E_i is a faithful edit of I_i according to y , and (ii) $\{E_i\}$ are multi-view consistent, i.e. there exists an underlying 3D scene representation \mathcal{S} whose renderings under poses $\{\pi_i\}$ yield $\{E_i\}$.

4.2. Score Distillation Sampling

Originally introduced in *DreamFusion* [50] for 3D generation using 2D diffusion models, **Score Distillation Sampling (SDS)** is an iterative technique for utilizing the generative prior of a pre-trained diffusion model ϵ_ψ (*teacher*) to tune the parameters θ of a differen-

tiable neural scene representation Φ_θ (*student*). At each iteration, the student is queried (rendered) through a differentiable operator g , yielding $\hat{\chi}_0 = g(\Phi_\theta)$. This prediction is then critiqued by the teacher, and the process repeats iteratively, updating θ until the student encodes a scene representation Φ_θ that yields plausible renderings.

The overall SDS framework, can be summarized as a five-stage pipeline, schematically shown in the inset figure:

1. Student Query. The student Φ_θ produces an image or latent $\hat{\chi}_0 = g(\Phi_\theta)$ to be critiqued. Commonly this is a differentiable rendering from a NeRF.

2. Student-Teacher Alignment. The student output $\hat{\chi}_0$ is mapped to the teacher’s input space as \hat{x}_0 , e.g., through an image encoder.

3. Perturbation. The aligned prediction \hat{x}_0 is perturbed according to the teacher’s forward diffusion process: $\hat{x}_t = \alpha_t \hat{x}_0 + \sigma_t \epsilon$, $\epsilon \sim \mathcal{N}(0, I)$.

4. Teacher Prediction. The teacher model ϵ_ψ processes \hat{x}_t (conditioned on an embedding y and the timestep t), and predicts the corresponding noise $\epsilon_\psi(\hat{x}_t; y, t)$.

5. Student Update. The residual between the sampled

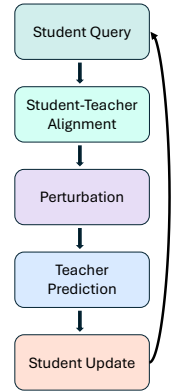


Figure 2. The five SDS stages.

noise ϵ and the teacher’s prediction defines the SDS gradient: $\nabla_{\theta} \mathcal{L}_{\text{SDS}} = \mathbb{E}_{t, \epsilon} [w(t) (\epsilon_{\psi}(\hat{x}_t; y, t) - \epsilon) \frac{\partial \hat{x}_0}{\partial \theta}]$, where $w(t)$ is a time-dependent weighting term. The gradient is backpropagated to update the student parameters θ .

SDS variants differ primarily in the specific design choice at each stage.

4.3. Consistent Sparse-View Editing Through Student Personalization

In our framework, where the student is a diffusion-based multi-view synthesis model, key SDS stages require specialized adaptations, which we detail in this subsection. Our proposed approach is illustrated in Figure 1.

Step 1: Student Query. In traditional SDS with NeRFs or 3DGS, the student prediction $\hat{\chi}_0 = g(\Phi_{\theta})$ is obtained via differentiable rendering. In our setting, the student is a multi-view diffusion model ϵ_{θ} , so the analogue is generating a sample via its denoising trajectory [24, 57]. Running a full sampling trajectory at each SDS iteration is however slow and computationally expensive, requiring backpropagation through many denoiser evaluations. Instead, we distill incrementally at each student timestep τ , starting from $\tau = T$ with latents sampled from the Gaussian distribution with student-scheduler specified variance $\{\zeta_{\text{T}}^i\}_{i=1}^N \sim \mathcal{N}(0, \sigma_{\text{S}}^2 I)$. We compute *single-step predictions* of the clean latents via the Tweedie formula [18]. These estimates $\{\hat{\zeta}_0^i(\tau)\}$ serve as intermediate student predictions to be critiqued by the teacher, shaping the student’s backward trajectory step by step.

Step 2: Student-Teacher Alignment. Although both student and teacher are latent diffusion models, they operate in different latent spaces and dimensions. A naive approach would decode the student’s predictions $\{\hat{\zeta}_0^i\}$ with its decoder \mathcal{D}_{S} and encode them with the teacher encoder \mathcal{E}_{T} before adding noise via the teacher’s forward process. However, backpropagating through both \mathcal{D}_{S} and \mathcal{E}_{T} would be prohibitively expensive. Inspired by prior work on convergent representations [2, 29, 36, 38], which suggests that simple mappings can often bridge the representation spaces of different networks, we instead resize the student’s latents to the teacher’s expected dimensions $(H_{\text{T}}, W_{\text{T}})$ via bilinear interpolation: $\hat{z}_0^i = \mathcal{I}_{\text{bilinear}}(\hat{\zeta}_0^i; H_{\text{T}}, W_{\text{T}})$. For our chosen models, this lightweight approach suffices, suggesting that the student latents implicitly align with the teacher’s latent space during fine-tuning.

Step 3: Perturbation. The mapped latents are perturbed using the teacher’s forward process $\hat{z}_t^i = \alpha_t \hat{z}_0^i + \sigma_t \epsilon_i$, $\epsilon_i \sim \mathcal{N}(0, I)$, yielding noisy latents $\{\hat{z}_t^i\}$. A key design choice is the teacher timestep t . In standard SDS [50], t is drawn uniformly from $[0.02, 0.98]$, avoiding extreme noise levels for numerical stability. This is ill-suited to our setting: early



Figure 3. Random Cross-View Attention effect when used for full teacher sampling.

student outputs (large τ) lie off the natural image manifold, so at low t values their diffused versions fall outside the teacher’s distribution, causing unstable guidance.

Annealed t schedules have also been explored [26, 43], and a natural variant is to match t with the student timestep τ . Yet this is too restrictive—when τ is small, forcing $t \approx \tau$ limits the teacher’s ability to provide corrective gradients. We instead use a stochastic schedule: $t \sim \text{TruncNorm}(\mu = b, \sigma = \frac{b-\tau}{f}, a = \tau, b = 0.95)$, where f controls skewness. Larger f concentrates probability near b , making it more likely for the teacher to operate at higher noise levels. The randomness ensures that the teacher provides strong gradients every few iterations, which we find highly effective for avoiding collapse to poor local minima. See Appendix A.1 for further details and visualizations.

Step 4: Teacher Prediction. A straightforward application of our framework would pass the perturbed latents $\{\hat{z}_t^i\}_{i=1}^N$ as a batch to the monocular teacher U-Net ϵ_{ψ} , which would then produce independent noise estimates for each latent. Backpropagating such conflicting signals into the student can weaken its multi-view prior, yielding inconsistent final edits. To address this, we introduce a lightweight Random Cross-View Attention (RCVAttn) mechanism that encourages the teacher to generate more consistent edits within each batch. Inspired by attention-based alignment work [33], we randomly select a *key frame* index $\kappa \sim U\{1, \dots, N\}$ at each iteration. Each frame i attends to the tokens of the key frame:

$$\text{RCVAttn}(Q, K, V, i) = \text{softmax}\left(\frac{Q_i K_{\kappa}^{\top}}{\sqrt{d}}\right) V_{\kappa}, \quad (1)$$

where d is the query/key dimensionality. Aligning all frames to query the key frame improves consistency substantially, aiding in retaining the student’s multi-view prior. Unlike expensive extended-attention methods [12, 20, 69], RCVAttn adds no computational overhead. While non-key frames may experience reduced quality, randomly selecting

Algorithm 1 I-Mix2Mix

```
1: Input:
2:  $\{I_i\}_{i=1}^N, \{\pi_i\}_{i=1}^N, y$   $\triangleright$  Images, poses, and text prompt
3:  $\epsilon_\psi, \epsilon_\theta$   $\triangleright$  Frozen teacher and trainable student
4:  $z_{\text{ref}} \leftarrow \mathcal{E}_S(\text{TeacherEdit}(I_{\text{ref}}, y))$ 
5: Initialize  $\zeta_T^i \sim \mathcal{N}(0, \sigma_S^2 I)$ 
6: for  $\tau = T, T - \Delta\tau, \dots, 0$  do
7:   for  $k$  steps do
8:      $\{\hat{\zeta}_0^i\} \leftarrow \epsilon_\theta(\{\zeta_\tau^i\}, z_{\text{ref}}, \{\pi_i\})$ 
9:      $\hat{z}_0^i \leftarrow \mathcal{I}_{\text{bilinear}}(\hat{\zeta}_0^i)$ 
10:     $t \sim \text{TruncNorm}(\mu=b, \sigma=\frac{b-\tau}{f}, a=\tau, b=0.95)$ 
11:     $\epsilon_i \sim \mathcal{N}(0, I)$ 
12:     $\hat{z}_t^i \leftarrow \alpha_t \hat{z}_0^i + \sigma_t \epsilon_i$ 
13:     $\kappa \sim U\{1, \dots, N\}$   $\triangleright$  Select keyframe
14:     $\{\tilde{\epsilon}_i\} \leftarrow \epsilon_\psi(\{\hat{z}_t^i\}; y, \{I_i\}, t)$   $\triangleright$  With RCVAtn
15:     $\nabla_\theta \mathcal{L}_{\text{SDS}} \leftarrow \frac{1}{N} \sum_i (\tilde{\epsilon}_i - \epsilon_i) \frac{\partial \hat{z}_0^i}{\partial \theta}$ 
16:     $\theta \leftarrow \text{OptimizerStep}(\theta, \nabla_\theta \mathcal{L}_{\text{SDS}})$ 
17:   end for
18:    $\{\zeta_{\tau-\Delta\tau}^i\} \leftarrow \text{StudentStep}(\{\zeta_\tau^i\}, z_{\text{ref}}, \{\pi_i\}, \Delta\tau)$ 
19: end for
20: Output:  $E_i \leftarrow \mathcal{D}_T(\hat{z}_0^i)$ 
```

κ ensures all frames occasionally serve as the key, preventing noticeable degradation. The effect of RCVAtn, when applied to full teacher sampling process, is shown in Fig. 3.

Step 5: Student Update. Finally, the difference between the sampled noise and the teacher’s prediction defines the guidance direction in the SDS objective:

$$\nabla_\theta \mathcal{L}_{\text{SDS}} = \frac{1}{N} \sum_{i=1}^N (\epsilon_\psi(\hat{z}_t^i; y, I_i, t) - \epsilon_i) \frac{\partial \hat{z}_0^i}{\partial \theta}, \quad (2)$$

which is backpropagated to update the student weights.

This completes a single distillation iteration at student timestep τ . We start at $\tau = T$ and repeat this process for k iterations, personalizing the student model at this timestep to the indented edit. The student then performs a sampling step with its scheduler, producing latents $\{\zeta_{\tau-\Delta\tau}^i\}$, where $\Delta\tau$ is the step size. Distillation resumes at $\tau - \Delta\tau$, repeating k updates before the next sampling step. This nested procedure continues until $\tau = 0$, yielding final edited views that are instruction-faithful and multi-view consistent.

Initialization. Our student model, SEVA, is an “ M in, N out” model with $M \geq 1$, meaning that the denoiser ϵ_θ requires at least one clean input latent in addition to the N noisy latents. As a preprocessing step, we randomly select one of the input frames $I_{\text{ref}} \in \{I_i\}$ and pass it through the 2D teacher editor to generate a valid reference edit E_{ref} . This edit is then encoded using SEVA’s frozen encoder to obtain a reference latent $z_{\text{ref}} = \mathcal{E}_S(E_{\text{ref}})$, which serves as the input frame to the denoiser in all distillation iterations. The framework is summarized in Algorithm 1.

5. Experiments

Methods in comparison. We compare with four widely used, open-source methods that also employ Instruct-Pix2Pix as the 2D editor, covering distinct paradigms for multi-view editing: *Instruct-NeRF2NeRF (I-N2N)* [22] and its 3DGS variant *Instruct-GS2GS (I-GS2GS)* [61] (both following the Iterative Dataset Update paradigm), *Text2Video-Zero (T2VZ)* [33] (a zero-shot image-to-video adaptation), and *DGE* [12] (extended attention for multi-view editing with 3DGS-based consolidation). Since I-N2N requires a trained NeRF, we optimize a Nerfacto [59] model on the N input views; similarly, because I-GS2GS and DGE require a 3DGS, we optimize a Splatfacto [59] model. All baselines are run with default settings from the official implementations or papers.

Evaluation. We evaluate our method on scenes from several datasets: I-N2N [22], Tanks and Temples [34], CO3D [53], and Mip-NeRF 360 [6]. Following prior protocols, for comparison with baselines we apply 20 edits to three standard test scenes from I-N2N (full edit set detailed in Appendix C); qualitative results on additional scenes appear in Appendix G. Per-frame edit quality and cross-view consistency are assessed with three CLIP-based [52] metrics commonly used in prior work [12, 14, 22]: (i) *CLIP Similarity*, the cosine similarity between an edited image and the prompt; (ii) *CLIP Directional Similarity* [7, 19], which measures alignment between prompt change and image change; (iii) *CLIP Directional Consistency* [22], which quantifies multi-view consistency by comparing the relative changes between pairs of original views O_i, O_j and their corresponding edited views E_i, E_j via $\cos\text{-sim}(\phi(O_i) - \phi(O_j), \phi(E_i) - \phi(E_j))$, where $\phi(\cdot)$ denotes the CLIP embedding. This metric captures whether the semantic difference between two views is preserved after editing. Unlike the original formulation, which considers only consecutive frames, we average over all $\binom{N}{2}$ pairs to account for our unordered, sparse-view setting.

We use $N = 4$ frames in main experiments, with additional results for larger N in Appendix H. Full implementation details, are detailed in Appendix A.

5.1. Comparison with Prior Work

Quantitative results are reported in Table 1, and representative qualitative comparisons are shown in Figure 4. Enlarged visualizations and additional examples are included in Appendix F.

Our method achieves the highest performance in *CLIP Directional Consistency (CLIP Cons.)*, indicating that edits remain more consistent across different views. Importantly, this does not come at the cost of per-frame edit quality, as demonstrated by CLIP Sim. and CLIP Dir. scores, where our method is either superior to or competitive with the baselines.

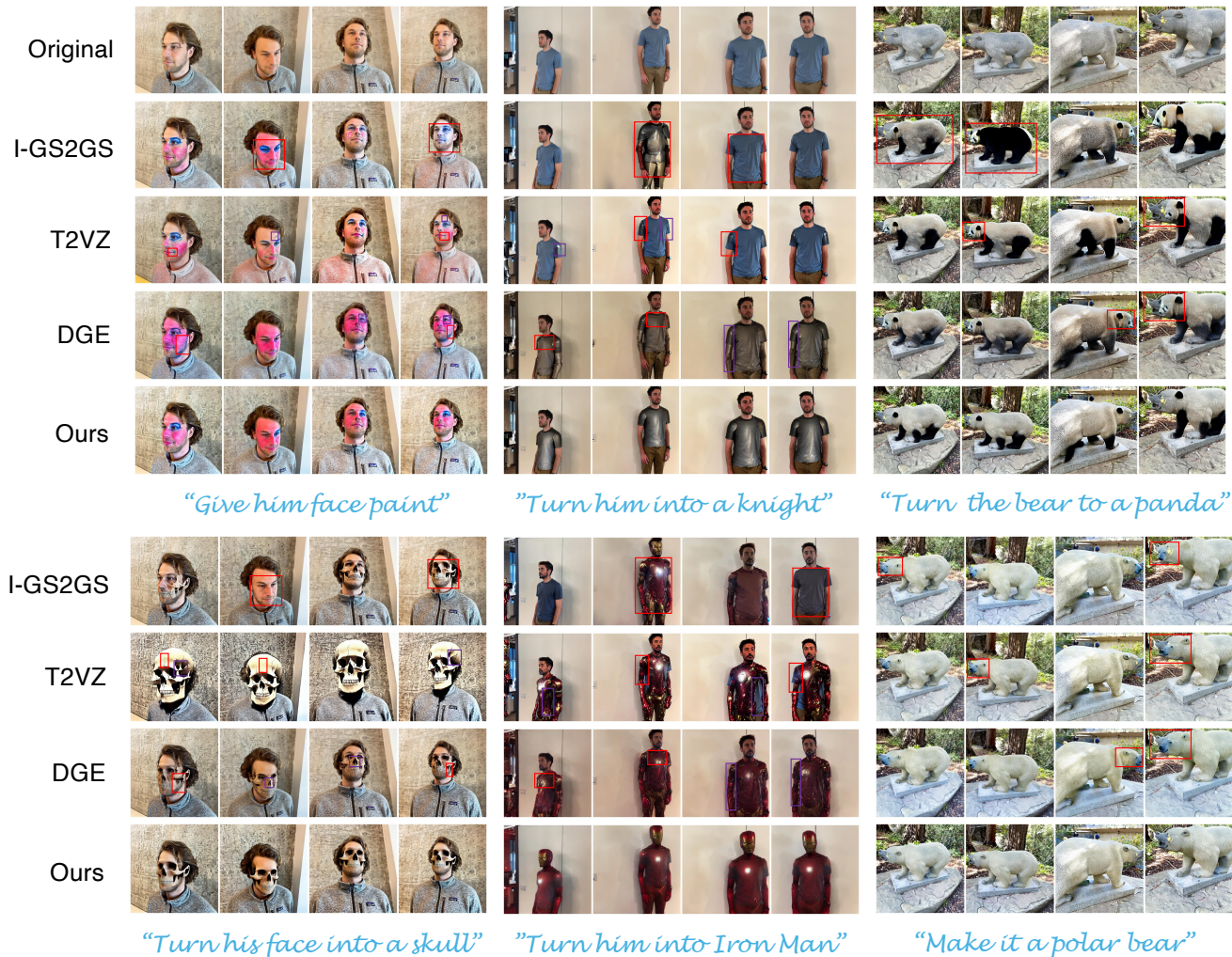


Figure 4. Qualitative comparison with prior work. The top row shows the original scenes, and the lower rows present edits from different methods. Matching red or purple rectangles indicate pairs of inconsistent regions, which frequently appear in baselines but not in our edits. Please zoom in electronically for details; enlarged views are provided in Appendix F.

Method	CLIP Cons. \uparrow	CLIP Sim. \uparrow	CLIP Dir. \uparrow
I-N2N	0.034	0.196	0.105
I-GS2GS	0.314	0.253	0.169
T2VZ	0.310	0.251	0.159
DGE	0.287	0.256	0.182
Ours	0.342	0.258	0.173

Table 1. Comparison of methods across view consistency, semantic alignment, and edit performance.

Notably, I-N2N fails completely in this sparse-view setting. We observed that Nerfacto struggles to fit the scene, producing severe floater artifacts even when rendering source poses. These distortions lie out of distribution

for the 2D editor, leading to unusable edits as shown in Appendix D.

The advantages of our approach compared to other baselines, are most clearly demonstrated qualitatively. In the sparse-view setting, baseline methods often struggle to maintain consistent edits across viewpoints due to two factors: (i) 3DGS-based consolidation becomes unreliable with limited views, as the 3DGS tends to overfit the training images [73, 77]; and (ii) cross-frame attention, while improving general appearance alignment, fails to enforce fine-grained consistency. Figure 4 illustrates these issues: I-GS2GS edits remain largely view-independent (e.g., the *Face Paint* edit), while T2VZ and DGE, though producing roughly appearance-consistent edits, introduce inconsistency in the details—such as mismatched sleeve and chest textures in the *Knight* and *Iron Man* edits, varying face paint

Method	# Inconsist. ↓	Scene Win % ↑	Consist. % ↑	Inconsist. % ↓
DGE	2.02	25.0	34.0	31.0
Ours	1.34	75.0	65.0	13.0

Table 2. Human study of multi-view consistency. Differences are statistically significant; full methodology appear in Appendix B.1.

SDS Stage	Config	CLIP Cons. ↑	CLIP Sim. ↑	CLIP Dir. ↑
–	Student Only	0.014	0.212	0.161
–	Teacher Only	0.228	0.252	0.184
Initialization (0)	Source ref. Frame	0.326	0.264	0.174
Alignment (2)	Learned Mapping	0.287	0.259	0.180
Perturbation (3)	Uniform t	0.363	0.260	0.146
	τ -matched t	0.435	0.231	0.107
Teacher Pred. (4)	W/O RCVAttn	0.230	0.260	0.175
	Full	0.337	0.263	0.178

Table 3. Ablation study evaluating different design choices. Weak results are highlighted in red.

colors and intensities in *Face Paint*, and view-dependent differences in *Skull* details such as the nose, cheek, and forehead. The lack of robust 3D consistency is especially evident in the *Bear* edit, which exhibits Janus-like multi-face artifacts. In contrast, I-Mix2Mix produces edits that are not only faithful to the instruction but also highly consistent across all views, without sacrificing image quality. This combination of instruction alignment, visual fidelity, and strong 3D consistency represents a clear improvement over existing approaches in the sparse-view setting.

Human survey. To further validate the 3D consistency advantage of I-Mix2Mix, we conducted a human survey comparing it to the strongest baseline, DGE. Raters were asked to identify and mark inconsistencies in the multi-view edited scenes produced by both algorithms. As shown in Table 2, I-Mix2Mix significantly outperforms DGE by producing fewer inconsistencies on average, achieving higher scene win percentages, and generating a greater proportion of "consistent" scenes (with 1 or fewer inconsistencies). Additionally, I-Mix2Mix results in far fewer "inconsistent" scenes (with 3 or more inconsistencies), demonstrating its superior multi-view consistency. See Appendix B.1 for full details of the methodology and statistical significance.

5.2. Ablation Study

We conduct an ablation study on 6 representative edits (listed in Appendix C) to assess the contributions of our design choices across the SDS pipeline. Quantitative results are summarized in Table 3, with particularly weak results highlighted in red. Our findings show that each component is essential to achieve both faithful edits and strong multi-view consistency.

Role of teacher and student. We first test the student and teacher models in isolation. In the *Student Only* setting, the student is given an edited frame as input and asked to sample additional views. This fails for several reasons: the student never sees the scene content captured by the other frames, leading to poor faithfulness; the SEVA prior struggles under single-view input; and we suspect that the edited scenes lie out-of-distribution for the model. This suggests that our approach *distills new capabilities into the student*, rather than simply searching within its existing sampling distribution. Conversely, in the *Teacher Only* setting, we rely on the teacher to edit each view independently. While individual frames adhere to the instruction edit, the lack of a 3D prior leads to severe cross-view inconsistency, as reflected by the low CLIP Consistency score. We present representative visualizations in Appendix E. We further ask whether a lightweight coupling could suffice: we adapt SDEdit [44] to our setting, using the teacher’s per-view edits as a coarse initialization for the multi-view student (Appendix E.1). In practice, this naïve fusion yields low-quality, view-inconsistent results. Together, these results confirm the necessity of distilling from the teacher into the student, rather than using either in isolation.

Initialization stage. In the *Source ref. Frame* setting, we input one of the original frames to the student encoder, to serve as the reference latent, without editing it first: $z_{\text{ref}} = \mathcal{E}_S(I_{\text{ref}})$. Skipping the reference frame edit negatively affected the distillation process, as the initial student predictions are further away from the target. This results in slightly lower multi-view consistency.

Alignment stage. Following findings in prior work on latent space alignment [29, 38], we replaced the bilinear interpolation with a learnable convolutional mapping (*Learned Mapping*), optimized during distillation, but found this brought no measurable benefit – the necessary transformation is likely captured during the fine-tuning of the student.

Perturbation stage. We evaluated two alternatives to our proposed forward schedule: *Uniform t* (similar to Poole et al. [50]), where t is sampled uniformly in $[0.05, 0.95]$, and *τ -matched t* , where the teacher’s timestep follows the student’s. Both variants tend to collapse to near-identity reconstructions of the input scene, which explains their paradoxically high CLIP Consistency: such outputs are trivially consistent but fail to realize the intended edit as reflected

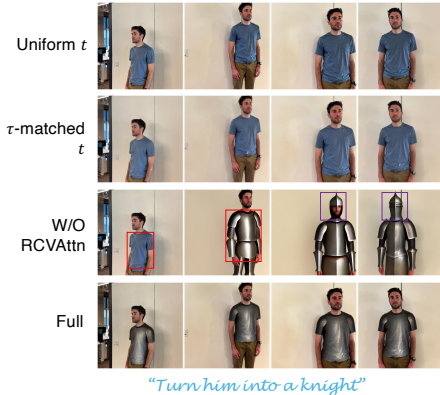


Figure 5. Failure cases from variants of the perturbation and teacher prediction stages. Rows 1–2: alternative forward schedules collapse to near-identity edits. Row 3: removing RCVAttn breaks multi-view coherence. Row 4: full method output.

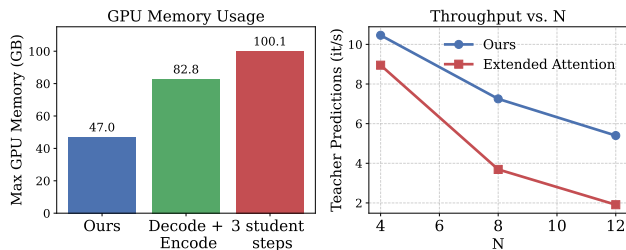


Figure 6. Efficiency analysis. Left: peak GPU memory usage for alternative student update and alignment strategies. Right: throughput degradation with extended attention as the number of views N increases.

in their low CLIP Directional scores. Visual examples are provided in the first two rows of Figure 5.

Teacher prediction stage. Disabling our Random Cross-View Attention mechanism (*W/O RCVAttn*) leads the teacher to process each perturbed latent independently. Without cross-view coupling, the student receives conflicting signals across views, leading to degraded multi-view consistency and breaking its 3D prior. This is again reflected in low CLIP Consistency, and illustrated in the third row of Figure 5.

Efficiency considerations. Several components of I-Mix2Mix were explicitly designed for memory and compute efficiency. Our choice of using a single-step prediction in the *Student Query* stage is crucial: a three-step alternative more than doubles peak memory usage for $N = 4$ views (Figure 6, left). In the *Student-Teacher Alignment* stage, interpolating latents rather than passing through the student’s decoder and teacher’s encoder reduces memory usage by over 40%. Finally, replacing the RCVAttn module with full extended attention significantly degraded throughput, worsening as the number of frames increased (Figure

6, right). We additionally experimented with fine-tuning the student using LoRA [25] rather than updating the full U-Net. While more parameter-efficient, this approach underperformed, and we leave the adaptation of lightweight variants to future work.

5.3. Beyond Image Editing

Our approach is not inherently limited to editing tasks. In principle, any pre-trained image-to-image diffusion model can serve as the teacher, with the multi-view student acting as a consolidator to produce a multi-view-to-multi-view solution. To explore this, we experimented with multi-view conditional generation. Specifically, we employed pre-trained ControlNets [74] as teachers to translate multiple depth maps or Canny edge maps of a 3D scene into consistent RGB images. Qualitative examples are provided in Appendix I. While the outputs were faithful to the conditioning inputs and maintained multi-view consistency, they often exhibited excessive blurriness—a known artifact of SDS-based optimization [50].

6. Discussion: Parallel to Diffusion Guidance

In standard diffusion guidance [3, 16], the model predictions at a given timestep are critiqued, and the resulting gradient is used to modify the sampling trajectory. In our framework, rather than applying such potentially unstable updates to the latents, we backpropagate the guidance signal to the *student’s weights*. This approach effectively transfers the teacher’s knowledge without making aggressive modifications to the latents themselves, avoiding divergence from the target distribution.

7. Conclusion, Limitations, and Future Work

We presented I-Mix2Mix, a novel framework for multi-view image editing that achieves high multi-view consistency in sparse-view settings, where prior methods typically fail. While effective, our approach inherits the limitations of its backbones, specifically InstructPix2Pix and SEVA, which can struggle with certain edit prompts or with maintaining perfect consistency across views. Given our framework’s modular nature, we anticipate that integrating stronger future backbones could mitigate these issues. Additionally, I-Mix2Mix requires multiple distillation iterations per noise level, making it more than twice as slow as our strongest competitor, DGE. We plan to explore strategies to reduce this overhead in future work. Finally, as discussed in Section 5.3, our framework is potentially general and applicable to a range of image manipulation tasks beyond editing. However, performance on these tasks currently lags behind our editing results, often producing blurry outputs. We leave the investigation of these directions to future work.

Acknowledgments. Or Litany acknowledges support from the Israel Science Foundation (grant 624/25) and the Azrieli Foundation Early Career Faculty Fellowship. This research was also supported in part by an academic gift from Meta. The authors gratefully acknowledge this support.

References

- [1] Mohammad Asim, Christopher Wewer, Thomas Wimmer, Bernt Schiele, and Jan Eric Lenssen. Met3r: Measuring multi-view consistency in generated images. In *Proceedings of the Computer Vision and Pattern Recognition Conference*, pages 6034–6044, 2025. 14
- [2] Andrea Asperti and Valerio Tonelli. Comparing the latent space of generative models. *Neural Computing and Applications*, 35(4):3155–3172, 2023. 4
- [3] Arpit Bansal, Hong-Min Chu, Avi Schwarzschild, Soumyadip Sengupta, Micah Goldblum, Jonas Geiping, and Tom Goldstein. Universal guidance for diffusion models. In *Proceedings of the IEEE/CVF conference on computer vision and pattern recognition*, pages 843–852, 2023. 8
- [4] Chong Bao, Yinda Zhang, Bangbang Yang, Tianxing Fan, Zesong Yang, Hujun Bao, Guofeng Zhang, and Zhaopeng Cui. Sine: Semantic-driven image-based nerf editing with prior-guided editing field. In *Proceedings of the IEEE/CVF Conference on Computer Vision and Pattern Recognition*, pages 20919–20929, 2023. 2
- [5] Roi Bar-On, Dana Cohen-Bar, and Daniel Cohen-Or. Editp23: 3d editing via propagation of image prompts to multi-view. *arXiv preprint arXiv:2506.20652*, 2025. 2
- [6] Jonathan T. Barron, Ben Mildenhall, Dor Verbin, Pratul P. Srinivasan, and Peter Hedman. Mip-nerf 360: Unbounded anti-aliased neural radiance fields. *CVPR*, 2022. 5, 16
- [7] Tim Brooks, Aleksander Holynski, and Alexei A Efros. Instructpix2pix: Learning to follow image editing instructions. In *Proceedings of the IEEE/CVF conference on computer vision and pattern recognition*, pages 18392–18402, 2023. 1, 2, 5, 14
- [8] Duygu Ceylan, Chun-Hao P Huang, and Niloy J Mitra. Pix2video: Video editing using image diffusion. In *Proceedings of the IEEE/CVF International Conference on Computer Vision*, pages 23206–23217, 2023. 2
- [9] Hansheng Chen, Ruoxi Shi, Yulin Liu, Bokui Shen, Jiayuan Gu, Gordon Wetzstein, Hao Su, and Leonidas Guibas. Generic 3d diffusion adapter using controlled multi-view editing. *arXiv preprint arXiv:2403.12032*, 2024. 2
- [10] Jun-Kun Chen, Jipeng Lyu, and Yu-Xiong Wang. Neuraleditor: Editing neural radiance fields via manipulating point clouds. In *Proceedings of the IEEE/CVF conference on computer vision and pattern recognition*, pages 12439–12448, 2023. 2
- [11] Minghao Chen, Junyu Xie, Iro Laina, and Andrea Vedaldi. Shap-editor: Instruction-guided latent 3d editing in seconds. *arXiv preprint arXiv:2312.09246*, 2023. 2
- [12] Minghao Chen, Iro Laina, and Andrea Vedaldi. Dge: Direct gaussian 3d editing by consistent multi-view editing. In *European Conference on Computer Vision*, pages 74–92. Springer, 2024. 2, 4, 5, 14
- [13] Yiwen Chen, Zilong Chen, Chi Zhang, Feng Wang, Xiaofeng Yang, Yikai Wang, Zhongang Cai, Lei Yang, Huaping Liu, and Guosheng Lin. Gaussianeditor: Swift and controllable 3d editing with gaussian splatting. In *Proceedings of the IEEE/CVF conference on computer vision and pattern recognition*, pages 21476–21485, 2024. 2
- [14] Yufeng Chi, Huimin Ma, Kafeng Wang, and Jianmin Li. Disco3d: Distilling multi-view consistency for 3d scene editing. *arXiv preprint arXiv:2508.01684*, 2025. 2, 5
- [15] Pei-Ze Chiang, Meng-Shiun Tsai, Hung-Yu Tseng, Wei-Sheng Lai, and Wei-Chen Chiu. Stylizing 3d scene via implicit representation and hypernetwork. In *Proceedings of the IEEE/CVF winter conference on applications of computer vision*, pages 1475–1484, 2022. 2
- [16] Hyungjin Chung, Jeongsol Kim, Michael T Mccann, Marc L Klasky, and Jong Chul Ye. Diffusion posterior sampling for general noisy inverse problems. *arXiv preprint arXiv:2209.14687*, 2022. 8
- [17] Jiahua Dong and Yu-Xiong Wang. Vica-nerf: View-consistency-aware 3d editing of neural radiance fields. *Advances in Neural Information Processing Systems*, 36: 61466–61477, 2023. 2
- [18] Bradley Efron. Tweedie’s formula and selection bias. *Journal of the American Statistical Association*, 106(496):1602–1614, 2011. 4
- [19] Rinon Gal, Or Patashnik, Haggai Maron, Amit H Bermano, Gal Chechik, and Daniel Cohen-Or. Stylegan-nada: Clip-guided domain adaptation of image generators. *ACM Transactions on Graphics (TOG)*, 41(4):1–13, 2022. 5
- [20] Michal Geyer, Omer Bar-Tal, Shai Bagon, and Tali Dekel. Tokenflow: Consistent diffusion features for consistent video editing. *arXiv preprint arXiv:2307.10373*, 2023. 2, 4
- [21] Eyal Gomel and Lior Wolf. Diffusion-based attention warping for consistent 3d scene editing, 2024. 2
- [22] Ayaan Haque, Matthew Tancik, Alexei A Efros, Aleksander Holynski, and Angjoo Kanazawa. Instruct-nerf2nerf: Editing 3d scenes with instructions. In *Proceedings of the IEEE/CVF international conference on computer vision*, pages 19740–19750, 2023. 1, 2, 5, 14, 15
- [23] Jonathan Ho and Tim Salimans. Classifier-free diffusion guidance. *arXiv preprint arXiv:2207.12598*, 2022. 2
- [24] Jonathan Ho, Ajay Jain, and Pieter Abbeel. Denoising diffusion probabilistic models. *Advances in neural information processing systems*, 33:6840–6851, 2020. 4
- [25] Edward J Hu, Yelong Shen, Phillip Wallis, Zeyuan Allen-Zhu, Yuanzhi Li, Shean Wang, Lu Wang, Weizhu Chen, et al. Lora: Low-rank adaptation of large language models. *ICLR*, 1(2):3, 2022. 8
- [26] Yukun Huang, Jianan Wang, Yukai Shi, Boshi Tang, Xianbiao Qi, and Lei Zhang. Dreamtime: An improved optimization strategy for diffusion-guided 3d generation. *arXiv preprint arXiv:2306.12422*, 2023. 4
- [27] Yufei Huang, Bangyan Liao, Yuqi Hu, Haitao Lin, Lirong Wu, Siyuan Li, Cheng Tan, Zicheng Liu, Yunfan Liu, Zelin Zang, et al. Dacapo: Score distillation as stacked bridge

- for fast and high-quality 3d editing. In *Proceedings of the Computer Vision and Pattern Recognition Conference*, pages 16304–16313, 2025. 2
- [28] Yi-Hua Huang, Yue He, Yu-Jie Yuan, Yu-Kun Lai, and Lin Gao. Stylizednerf: consistent 3d scene stylization as stylized nerf via 2d-3d mutual learning. In *Proceedings of the IEEE/CVF conference on computer vision and pattern recognition*, pages 18342–18352, 2022. 2
- [29] Minyoung Huh, Brian Cheung, Tongzhou Wang, and Phillip Isola. The platonic representation hypothesis. *arXiv preprint arXiv:2405.07987*, 2024. 4, 7
- [30] Lihan Jiang, Yucheng Mao, Linning Xu, Tao Lu, Kerui Ren, Yichen Jin, Xudong Xu, Mulin Yu, Jiangmiao Pang, Feng Zhao, et al. Anysplat: Feed-forward 3d gaussian splatting from unconstrained views. *arXiv preprint arXiv:2505.23716*, 2025. 14
- [31] Hiromichi Kamata, Yuiko Sakuma, Akio Hayakawa, Masato Ishii, and Takuya Narihira. Instruct 3d-to-3d: Text instruction guided 3d-to-3d conversion. *arXiv preprint arXiv:2303.15780*, 2023. 1, 2
- [32] Bernhard Kerbl, Georgios Kopanas, Thomas Leimkühler, and George Drettakis. 3d gaussian splatting for real-time radiance field rendering. *ACM Transactions on Graphics*, 42(4), 2023. 1, 2
- [33] Levon Khachatryan, Andranik Movsisyan, Vahram Tadevosyan, Roberto Henschel, Zhangyang Wang, Shant Navasardyan, and Humphrey Shi. Text2video-zero: Text-to-image diffusion models are zero-shot video generators. In *Proceedings of the IEEE/CVF International Conference on Computer Vision*, pages 15954–15964, 2023. 2, 4, 5
- [34] Arno Knapitsch, Jaesik Park, Qian-Yi Zhou, and Vladlen Koltun. Tanks and temples: Benchmarking large-scale scene reconstruction. *ACM Transactions on Graphics*, 36(4), 2017. 5, 16
- [35] Black Forest Labs, Stephen Batifol, Andreas Blattmann, Frederic Boesel, Saksham Consul, Cyril Diagne, Tim Dockhorn, Jack English, Zion English, Patrick Esser, et al. Flux. 1 kontext: Flow matching for in-context image generation and editing in latent space. *arXiv preprint arXiv:2506.15742*, 2025. 2
- [36] Karel Lenc and Andrea Vedaldi. Understanding image representations by measuring their equivariance and equivalence. In *Proceedings of the IEEE conference on computer vision and pattern recognition*, pages 991–999, 2015. 4
- [37] Ruihuang Li, Liyi Chen, Zhengqiang Zhang, Varun Jampani, Vishal M Patel, and Lei Zhang. Syncnoise: Geometrically consistent noise prediction for instruction-based 3d editing. In *Proceedings of the AAAI Conference on Artificial Intelligence*, pages 4905–4913, 2025. 2
- [38] Yixuan Li, Jason Yosinski, Jeff Clune, Hod Lipson, and John Hopcroft. Convergent learning: Do different neural networks learn the same representations? *arXiv preprint arXiv:1511.07543*, 2015. 4, 7
- [39] Yuhan Li, Yishun Dou, Yue Shi, Yu Lei, Xuanhong Chen, Yi Zhang, Peng Zhou, and Bingbing Ni. Focaldreamer: Text-driven 3d editing via focal-fusion assembly. In *Proceedings of the AAAI conference on artificial intelligence*, pages 3279–3287, 2024. 1, 2
- [40] Steven Liu, Xiuming Zhang, Zhoutong Zhang, Richard Zhang, Jun-Yan Zhu, and Bryan Russell. Editing conditional radiance fields. In *Proceedings of the IEEE/CVF international conference on computer vision*, pages 5773–5783, 2021. 2
- [41] Shaoteng Liu, Yuechen Zhang, Wenbo Li, Zhe Lin, and Jiaya Jia. Video-p2p: Video editing with cross-attention control. In *Proceedings of the IEEE/CVF Conference on Computer Vision and Pattern Recognition*, pages 8599–8608, 2024. 2
- [42] Ilya Loshchilov and Frank Hutter. Decoupled weight decay regularization. *arXiv preprint arXiv:1711.05101*, 2017. 14
- [43] Artem Lukoianov, Haitz Sáez de Ocáriz Borde, Kristjan Greenewald, Vitor Guizilini, Timur Bagautdinov, Vincent Sitzmann, and Justin M Solomon. Score distillation via reparametrized ddim. *Advances in Neural Information Processing Systems*, 37:26011–26044, 2024. 4
- [44] Chenlin Meng, Yutong He, Yang Song, Jiaming Song, Jiajun Wu, Jun-Yan Zhu, and Stefano Ermon. Sdedit: Guided image synthesis and editing with stochastic differential equations. *arXiv preprint arXiv:2108.01073*, 2021. 7, 15
- [45] Aryan Mikaeili, Or Perel, Mehdi Safaee, Daniel Cohen-Or, and Ali Mahdavi-Amiri. Sked: Sketch-guided text-based 3d editing. In *Proceedings of the IEEE/CVF International Conference on Computer Vision*, pages 14607–14619, 2023. 2
- [46] Ben Mildenhall, Pratul P Srinivasan, Matthew Tancik, Jonathan T Barron, Ravi Ramamoorthi, and Ren Ng. Nerf: Representing scenes as neural radiance fields for view synthesis. *Communications of the ACM*, 65(1):99–106, 2021. 1, 2
- [47] Ashkan Mirzaei, Tristan Aumentado-Armstrong, Konstantinos G Derpanis, Jonathan Kelly, Marcus A Brubaker, Igor Gilitschenski, and Alex Levinshtein. Spin-nerf: Multiview segmentation and perceptual inpainting with neural radiance fields. In *Proceedings of the IEEE/CVF Conference on Computer Vision and Pattern Recognition*, pages 20669–20679, 2023. 2
- [48] Thu Nguyen-Phuoc, Feng Liu, and Lei Xiao. Snerf: stylized neural implicit representations for 3d scenes. *arXiv preprint arXiv:2207.02363*, 2022. 2
- [49] Maria Parelli, Michael Oechsle, Michael Niemeyer, Federico Tombari, and Andreas Geiger. 3d-latte: Latent space 3d editing from textual instructions. *arXiv preprint arXiv:2509.00269*, 2025. 2
- [50] Ben Poole, Ajay Jain, Jonathan T Barron, and Ben Mildenhall. Dreamfusion: Text-to-3d using 2d diffusion. *arXiv preprint arXiv:2209.14988*, 2022. 1, 2, 3, 4, 7, 8, 16
- [51] Chenyang Qi, Xiaodong Cun, Yong Zhang, Chenyang Lei, Xintao Wang, Ying Shan, and Qifeng Chen. Fatezero: Fusing attentions for zero-shot text-based video editing. In *Proceedings of the IEEE/CVF International Conference on Computer Vision*, pages 15932–15942, 2023. 2
- [52] Alec Radford, Jong Wook Kim, Chris Hallacy, Aditya Ramesh, Gabriel Goh, Sandhini Agarwal, Girish Sastry, Amanda Askell, Pamela Mishkin, Jack Clark, et al. Learning transferable visual models from natural language supervision. In *International conference on machine learning*, pages 8748–8763. Pmlr, 2021. 5

- [53] Jeremy Reizenstein, Roman Shapovalov, Philipp Henzler, Luca Sbordone, Patrick Labatut, and David Novotny. Common objects in 3d: Large-scale learning and evaluation of real-life 3d category reconstruction. In *Proceedings of the IEEE/CVF international conference on computer vision*, pages 10901–10911, 2021. 5, 15
- [54] Robin Rombach, Andreas Blattmann, Dominik Lorenz, Patrick Esser, and Björn Ommer. High-resolution image synthesis with latent diffusion models. In *Proceedings of the IEEE/CVF conference on computer vision and pattern recognition*, pages 10684–10695, 2022. 2
- [55] Etai Sella, Gal Fiebelman, Peter Hedman, and Hadar Averbuch-Elor. Vox-e: Text-guided voxel editing of 3d objects. In *Proceedings of the IEEE/CVF international conference on computer vision*, pages 430–440, 2023. 2
- [56] Chaehun Shin, Heeseung Kim, Che Hyun Lee, Sang-gil Lee, and Sungroh Yoon. Edit-a-video: Single video editing with object-aware consistency. In *Asian Conference on Machine Learning*, pages 1215–1230. PMLR, 2024. 2
- [57] Jiaming Song, Chenlin Meng, and Stefano Ermon. Denoising diffusion implicit models. *arXiv preprint arXiv:2010.02502*, 2020. 4
- [58] Saar Stern, Ido Sobol, and Or Litany. Appreciate the view: A task-aware evaluation framework for novel view synthesis, 2025. 14
- [59] Matthew Tancik, Ethan Weber, Evonne Ng, Ruilong Li, Brent Yi, Terrance Wang, Alexander Kristoffersen, Jake Austin, Kamyar Salehi, Abhik Ahuja, et al. Nerfstudio: A modular framework for neural radiance field development. In *ACM SIGGRAPH 2023 conference proceedings*, pages 1–12, 2023. 5, 15
- [60] Zeng Tao, Zheng Ding, Zeyuan Chen, Xiang Zhang, Leizhi Li, and Zhuowen Tu. C3editor: Achieving controllable consistency in 2d model for 3d editing. *arXiv preprint arXiv:2510.04539*, 2025. 2
- [61] Cyrus Vachha and Ayaan Haque. Instruct-gs2gs: Editing 3d gaussian splats with instructions, 2024. 1, 2, 5
- [62] Patrick von Platen, Suraj Patil, Anton Lozhkov, Pedro Cuenca, Nathan Lambert, Kashif Rasul, Mishig Davaadorj, Dhruv Nair, Sayak Paul, Steven Liu, William Berman, Yiyi Xu, and Thomas Wolf. Diffusers: State-of-the-art diffusion models. 14
- [63] Binglun Wang, Niladri Shekhar Dutt, and Niloy J Mitra. Pro-teusnerf: Fast lightweight nerf editing using 3d-aware image context. *Proceedings of the ACM on Computer Graphics and Interactive Techniques*, 7(1):1–17, 2024. 2
- [64] Can Wang, Menglei Chai, Mingming He, Dongdong Chen, and Jing Liao. Clip-nerf: Text-and-image driven manipulation of neural radiance fields. In *Proceedings of the IEEE/CVF conference on computer vision and pattern recognition*, pages 3835–3844, 2022. 2
- [65] Can Wang, Ruixiang Jiang, Menglei Chai, Mingming He, Dongdong Chen, and Jing Liao. Nerf-art: Text-driven neural radiance fields stylization. *IEEE Transactions on Visualization and Computer Graphics*, 30(8):4983–4996, 2023. 2
- [66] Junjie Wang, Jiemin Fang, Xiaopeng Zhang, Lingxi Xie, and Qi Tian. Gaussianeditor: Editing 3d gaussians delicately with text instructions. In *Proceedings of the IEEE/CVF conference on computer vision and pattern recognition*, pages 20902–20911, 2024. 2
- [67] Shuzhe Wang, Vincent Leroy, Yohann Cabon, Boris Chidlovskii, and Jerome Revaud. Dust3r: Geometric 3d vision made easy. In *Proceedings of the IEEE/CVF Conference on Computer Vision and Pattern Recognition*, pages 20697–20709, 2024. 14
- [68] Silvan Weder, Guillermo Garcia-Hernando, Aron Monszpart, Marc Pollefeys, Gabriel J Brostow, Michael Firman, and Sara Vicente. Removing objects from neural radiance fields. In *Proceedings of the IEEE/CVF Conference on Computer Vision and Pattern Recognition*, pages 16528–16538, 2023. 2
- [69] Jay Zhangjie Wu, Yixiao Ge, Xintao Wang, Stan Weixian Lei, Yuchao Gu, Yufei Shi, Wynne Hsu, Ying Shan, Xiao-hu Qie, and Mike Zheng Shou. Tune-a-video: One-shot tuning of image diffusion models for text-to-video generation. In *Proceedings of the IEEE/CVF international conference on computer vision*, pages 7623–7633, 2023. 2, 4
- [70] Ruihao Xia, Yang Tang, and Pan Zhou. Towards scalable and consistent 3d editing. *arXiv preprint arXiv:2510.02994*, 2025. 2
- [71] Bangbang Yang, Yinda Zhang, Yinghao Xu, Yijin Li, Han Zhou, Hujun Bao, Guofeng Zhang, and Zhaopeng Cui. Learning object-compositional neural radiance field for editable scene rendering. In *Proceedings of the IEEE/CVF international conference on computer vision*, pages 13779–13788, 2021. 2
- [72] Yu-Jie Yuan, Yang-Tian Sun, Yu-Kun Lai, Yuewen Ma, Rongfei Jia, and Lin Gao. Nerf-editing: geometry editing of neural radiance fields. In *Proceedings of the IEEE/CVF conference on computer vision and pattern recognition*, pages 18353–18364, 2022. 2
- [73] Jiawei Zhang, Jiahe Li, Xiaohan Yu, Lei Huang, Lin Gu, Jin Zheng, and Xiao Bai. Cor-gs: sparse-view 3d gaussian splatting via co-regularization. In *European Conference on Computer Vision*, pages 335–352. Springer, 2024. 2, 6
- [74] Lvmin Zhang, Anyi Rao, and Maneesh Agrawala. Adding conditional control to text-to-image diffusion models. In *Proceedings of the IEEE/CVF international conference on computer vision*, pages 3836–3847, 2023. 8, 16
- [75] Canyu Zhao, Xiaoman Li, Tianjian Feng, Zhiyue Zhao, Hao Chen, and Chunhua Shen. Tinker: Diffusion’s gift to 3d-multi-view consistent editing from sparse inputs without per-scene optimization. *arXiv preprint arXiv:2508.14811*, 2025. 2
- [76] Jensen Jinghao Zhou, Hang Gao, Vikram Voleti, Aaryaman Vasishtha, Chun-Han Yao, Mark Boss, Philip Torr, Christian Rupprecht, and Varun Jampani. Stable virtual camera: Generative view synthesis with diffusion models. *arXiv preprint arXiv:2503.14489*, 2025. 1, 2, 14
- [77] Zehao Zhu, Zhiwen Fan, Yifan Jiang, and Zhangyang Wang. Fsgs: Real-time few-shot view synthesis using gaussian splatting. In *European conference on computer vision*, pages 145–163. Springer, 2024. 2, 6
- [78] Zhe Zhu, Honghua Chen, Peng Li, and Mingqiang Wei. Coreeditor: Consistent 3d editing via correspondence-

constrained diffusion. *arXiv preprint arXiv:2508.11603*, 2025. [2](#)

- [79] Jingyu Zhuang, Chen Wang, Liang Lin, Lingjie Liu, and Guanbin Li. Dreameditor: Text-driven 3d scene editing with neural fields. In *SIGGRAPH Asia 2023 Conference Papers*, pages 1–10, 2023. [2](#)

Contents

1. Introduction	1
2. Related Works	2
3. Preliminaries	2
4. Method	2
4.1. Problem Formulation	3
4.2. Score Distillation Sampling	3
4.3. Consistent Sparse-View Editing Through Student Personalization	4
5. Experiments	5
5.1. Comparison with Prior Work	5
5.2. Ablation Study	7
5.3. Beyond Image Editing	8
6. Discussion: Parallel to Diffusion Guidance	8
7. Conclusion, Limitations, and Future Work	8
Appendix Overview	13
A Implementation Details	14
A.1. Teacher Forward Schedule	14
B 3D Consistency Evaluation	14
B.1. Human Survey	14
C Evaluation Scenes and Edits	15
D Limitations of Instruct-NeRF2NeRF in Sparse-View Settings	15
E Student and Teacher Limitations	15
E.1. SDEdit-Style Fusion Without Distillation	15
F. Extended Qualitative Comparisons with Baselines	15
G Additional Results on Diverse Scenes	15
H Results with More Input Frames	16
I. Beyond Image Editing	16
J. Use of Large Language Models	16

A. Implementation Details

We use SEVA 1.1 [76] as the pre-trained student model and InstructPix2Pix [7] from the Diffusers library [62] as the frozen teacher. Consistent with prior observations [12, 22], the teacher’s classifier-free guidance (CFG) scales for both prompt and input image have a significant effect on the *degree of edit intensity*—a factor that is often subjective and a matter of personal taste. For most edits we adopt the default $S_T = 7.5$ for the prompt and $S_I = 1.5$ for the input image, with adjustments detailed appendix C. We perform distillation over 40 student timesteps ($\Delta\tau = \frac{1}{40}$), with $k = 50$ updates per step. Optimization is done with AdamW [42], using a maximum learning rate of 1×10^{-4} after 200 iterations of linear warm-up, followed by cosine decay down to 5×10^{-5} . This yields just over 2000 distillation iterations per experiment, which take about 40 minutes on a single NVIDIA H200 GPU. The input frames are selected randomly.

A.1. Teacher Forward Schedule

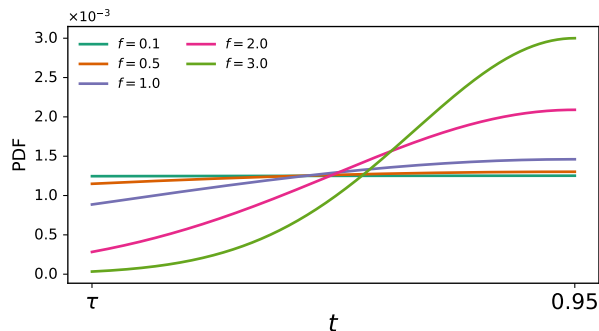


Figure 7. Teacher timestep schedule for different skewness factors f .

We employ a stochastic schedule for the teacher forward process, sampling timesteps as

$$t \sim \text{TruncNorm}(\mu = b, \sigma = (b - \tau)/f, a = \tau, b = 0.95),$$

where τ is the current student timestep and f controls the skewness of the distribution. Larger f concentrates probability near b , making the teacher more likely to operate at higher noise levels. The stochasticity ensures the teacher provides strong gradients every few iterations, which we find effective for avoiding collapse to poor local minima. Figure 7 illustrates how different f values shape the probability distribution. In practice, we use $f = 0.5$, yielding an approximately uniform distribution over $[\tau, 0.95]$.

B. 3D Consistency Evaluation

A strong multi-view generative model should produce image sequences in which each frame is individually high-quality and the *entire sequence* is 3D consistent. Unlike image quality or reconstruction accuracy, however, there is currently no widely accepted metric for evaluating 3D consistency. Recent work has begun to address this gap, but existing approaches remain limited.

MEt3R [1] leverages Dust3r [67] to obtain dense 3D reconstructions for pairs of images in a sequence, and measures feature-space reprojection errors in overlapping regions to assess consistency. While promising, this approach is not well suited to our *sparse-view* setting, where overlapping content between images is minimal. PRISM [58] instead uses diffusion features that capture source–target viewpoint relationships and is, in principle, better suited to large viewpoint changes, but its current implementation is restricted to object-centric scenes.

We also explored using recent feed-forward 3D reconstruction models to lift an evaluated sequence into 3D and measure reprojection error. The underlying assumption is that 3D-consistent scenes should yield lower reprojection error than inconsistent ones. To this end, we employed AnySplat [30] as the sparse-view reconstruction model. While its performance is impressive, it proved insufficient for our purposes: even 3D-consistent edited scenes—and occasionally ground-truth scenes—produced high reconstruction error. This may be due both to the inherent difficulty of the sparse-view setting and to edited scenes falling outside the model’s training distribution.

Given these limitations, we adopt the **CLIP Directional Consistency** metric introduced in prior 3D editing work [22], as detailed in Section 5. To complement this automatic metric, we additionally conduct a user study, described in the following subsection.

B.1. Human Survey

Protocol. We compare I-Mix2Mix against the strongest baseline, DGE, in a human study focused solely on *multi-view consistency*. Each rating task shows a set of four images from the same edited scene. Raters are instructed to mark every inconsistency they observe by placing *one pair of rectangles* on the contradictory areas in two views that disagree (each pair counts as one inconsistency). Figure 23 presents an example of the inconsistencies marked by a rater. Each algorithm produces 20 edited scenes (from Table 4), resulting in 40 total sets of images. On average, each set receives 5 independent ratings, for a total of 200 rated tasks (100 per algorithm).

Primary metric. For each rated task we gather the *number of inconsistency pairs* (two rectangles), denoted #Pairs.

Lower is better (fewer inconsistencies).

Aggregate comparisons. We report four metrics (Table 2): (i) **# Inconsistencies**—mean #Pairs per task; (ii) **Scene Win %**—fraction of scenes where an algorithm’s scene mean #Pairs is lower than the competitor; (iii) **Consistent %**—fraction of task ratings with #Pairs ≤ 1 ; (iv) **Inconsistent %**—fraction with #Pairs ≥ 3 .

Statistical tests. Because per-set sample sizes are small, we avoid normality assumptions and use non-parametric or exact tests:

- **Paired by scene #Pairs means:** two-sided sign-flip permutation test on per-scene difference of means (20 scenes, 20,000 randomizations). Result: $\bar{\Delta} = \text{mean}(\text{I-Mix2Mix} - \text{DGE}) = -0.5607$, two-sided $p = 0.0371$.
- **Scene wins:** exact binomial sign test on wins. I-Mix2Mix wins 15/20 scenes; one-sided $p = 0.020695$ (testing I-Mix2Mix $>$ DGE), two-sided $p = 0.041389$.
- **Rates (#Pairs ≤ 1 and #Pairs ≥ 3):** Fisher’s exact test on 2×2 counts (algorithm \times indicator). For *Consistent* (≤ 1): I-Mix2Mix 65/100 vs. DGE 34/100; two-sided $p = 1.9 \times 10^{-5}$, one-sided (I-Mix2Mix $>$ DGE) $p = 1.0 \times 10^{-5}$. For *Inconsistent* (≥ 3): I-Mix2Mix 13/100 vs. DGE 31/100; two-sided $p = 0.003405$, one-sided (I-Mix2Mix $<$ DGE) $p = 0.001703$.

Takeaway. Across all analyses, I-Mix2Mix exhibits fewer inconsistencies on average, wins on most scenes, substantially more highly consistent ratings (≤ 1), and far fewer inconsistent ratings (≥ 3). All reported advantages are statistically significant under the non-parametric / exact tests above.

C. Evaluation Scenes and Edits

We detail in Table 4 the edits used in our evaluations, applied to the standard Face, Bear, and Person scenes from the Instruct-NeRF2NeRF dataset [22]. The *Edit Prompt* is the editing instruction provided as input to the evaluated methods, while the *Original Prompt* and *Edited Prompt* are employed for CLIP-based evaluation. For each edit, we also report the teacher’s text and image CFG scales, s_T and s_I , used in quantitative evaluation. Edits with bolded prompts indicate those selected for the ablation experiments.

D. Limitations of Instruct-NeRF2NeRF in Sparse-View Settings

In the sparse-view regime, Instruct-NeRF2NeRF (I-N2N) [22] fails to produce coherent results. Its underlying Nerfacto [59] model, trained with default configurations for

30K iterations, struggles to reconstruct the scene accurately, generating severe floater artifacts even when rendering the original input poses. These distortions fall far outside the distribution expected by the 2D editor, rendering the resulting edits unusable. Figure 8 illustrates two representative examples of such failures, corresponding to the *Clown* and *Face Paint* edits.

E. Student and Teacher Limitations

Figure 9 illustrates the limitations of the student (SEVA) and teacher (Instruct-Pix2Pix) when used individually. Even on the unedited scene, SEVA can struggle to produce high-quality results with only a single input frame, as shown in the second row. When used as an editing baseline—receiving a single edited frame and asked to generate the remaining views—it fails to produce coherent frames (third row). Individual predictions from the teacher (final row) are independent across views, resulting in inconsistent and sometimes implausible edits.

E.1. SDEdit-Style Fusion Without Distillation

We test a simple, distillation-free fusion of the 2D editing teacher with the multi-view student by adapting SDEdit [44] to our setting. (1) We first produce per-view edits by independently sampling the teacher. (2) Each edited image is mapped into the student’s latent space by decoding with the teacher’s decoder and re-encoding with the student’s encoder. (3) We perturb these latents using the student’s forward diffusion process at noise levels $t \in \{0.25, 0.5, 0.75\}$. (4) Finally, we denoise with the multi-view student, conditioning on the edited view as the input latent (see Section 4). In principle, the teacher’s edits provide a semantic initialization while the student enforces multi-view consistency.

In practice, this SDEdit-style initialization fails to produce coherent multi-view results: edits are low-quality and inconsistent across views for all tested t (see Figure 10). This ablation underscores the need for explicit distillation, as implemented in I-Mix2Mix.

F. Extended Qualitative Comparisons with Baselines

In Figures 11, 12, 13, 14, 15, 16, 17, 18, we present additional qualitative comparisons to prior methods, including both enlarged versions of the edits shown in Figure 4 and additional edits. Matching red or purple rectangles highlight regions with multi-view inconsistencies.

G. Additional Results on Diverse Scenes

In Figures 19, 20 we present further qualitative results of I-Mix2Mix applied to four different scenes: *Car* from the CO3D dataset [53], *Garden* from the Mip-NeRF 360

Scene	Original Prompt	Edit Prompt	Edited Prompt	Text CFG	Image CFG
Face	"A man with curly hair in a grey jacket"	"Give him a Venetian mask"	"A man with curly hair in a grey jacket with a Venetian mask"	7.5	1.5
		"Turn him into a vampire"	"A vampire with curly hair"	7.5	1.5
		"Turn him into Tolkien Elf"	"A Tolkien Elf with curly hair"	9.0	1.5
		"Turn him into batman"	"A batman"	7.5	1.5
		"Turn his face into a skull"	"A man with a skull head in a grey jacket"	7.5	1.5
		"Turn him into Albert Einstein"	"Albert Einstein with curly hair"	7.5	1.5
		"Turn it to a Van Gogh painting"	"A Van Gogh painting of a man with curly hair in a jacket"	7.5	1.5
		"Give him face paint"	"A man with curly hair in a grey jacket with face paint"	7.5	1.5
Bear	"A stone bear in a garden"	"Turn the bear to a panda bear"	"A panda bear in a garden"	6.0	1.5
		"Turn the bear to a polar bear"	"A polar bear in a garden"	6.0	1.5
		"Turn the bear to a grizzly bear"	"A grizzly bear in a garden"	5.5	1.5
		"Turn the bear to a wooden bear"	"A wooden bear in a garden"	8.5	1.5
Person	"A man standing next to a wall wearing a blue T-shirt and brown pants"	"Turn him into Iron Man"	"An Iron Man standing next to a wall"	7.5	1.5
		"Turn the man into a robot"	"A robot standing next to a wall"	5.5	1.8
		"Make him in a suit"	"A man standing next to a wall wearing a suit"	6.5	1.8
		"Turn him into a clown"	"A clown standing next to a wall"	6.0	1.8
		"Make him into a marble statue"	"A marble statue of a man next to a wall"	7.5	1.5
		"Turn him into a cowboy with a hat"	"A cowboy wearing a hat standing next to a wall"	6.0	1.5
		"Turn him into a soldier"	"A soldier standing next to a wall"	7.5	1.5
		"Turn him into a knight"	"A knight standing next to a wall"	6.0	1.5

Table 4. Prompts and CFG values for each edit used for quantitative evaluation.

dataset [6], and *Horse* and *Ignatius* from the Tanks and Temples dataset [34].

H. Results with More Input Frames

Figure 21 presents outputs of I-Mix2Mix when using $N = 8$ input frames.

I. Beyond Image Editing

I-Mix2Mix is not tied to a specific editor or to editing tasks, and can in principle generalize to other multi-view conditional generation scenarios. To illustrate this, we used pre-trained ControlNets [74] as teachers to translate multiple

depth or Canny maps of a 3D scene into consistent RGB images. Figure 22 shows examples. While outputs respect the conditioning and maintain multi-view consistency, they often appear overly blurry, highlighting limitations of SDS-based optimization [50].

J. Use of Large Language Models

Large language models were employed as general-purpose assistants for both writing and coding throughout this work.

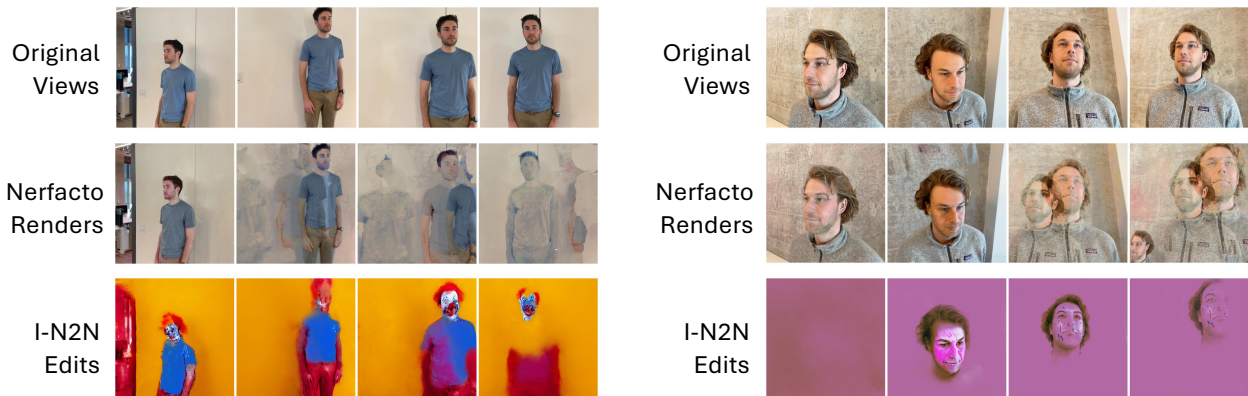


Figure 8. Examples for I-N2N failures in the sparse-view setting.

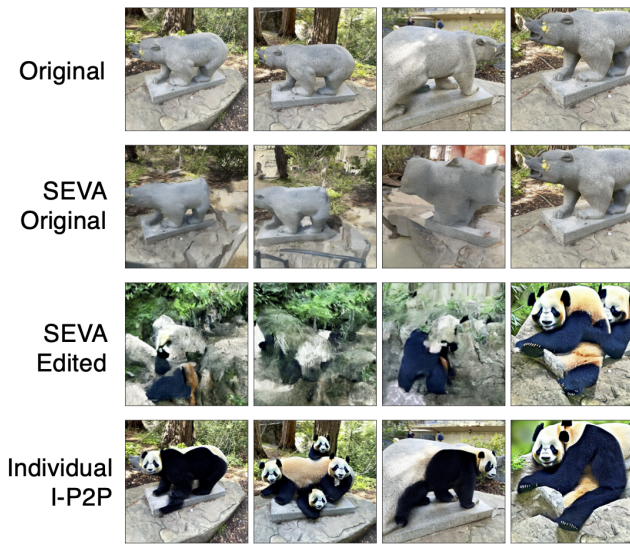


Figure 9. Student and Teacher models limitation example, on the *Bear* scene and *Panda* edit.

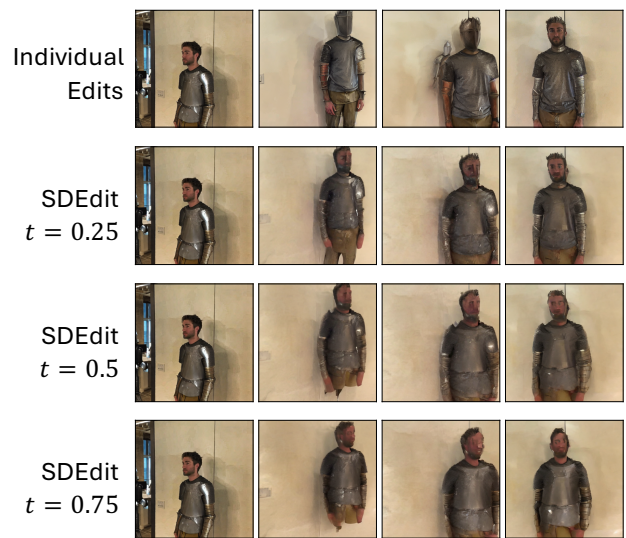


Figure 10. SDEdit failure example, on the *Person* scene and *Knight* edit.

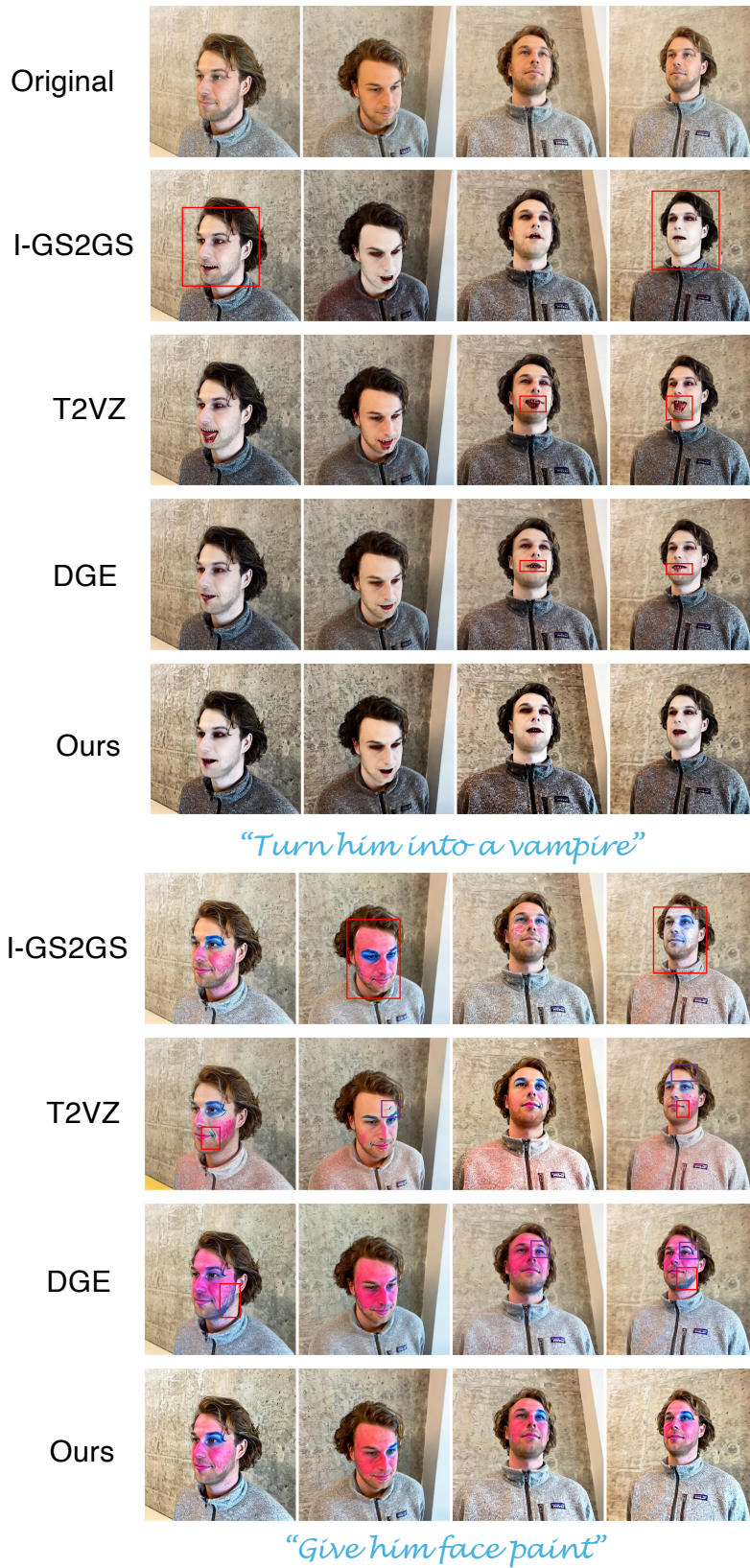


Figure 11. Comparison to baselines on Face scene edits.

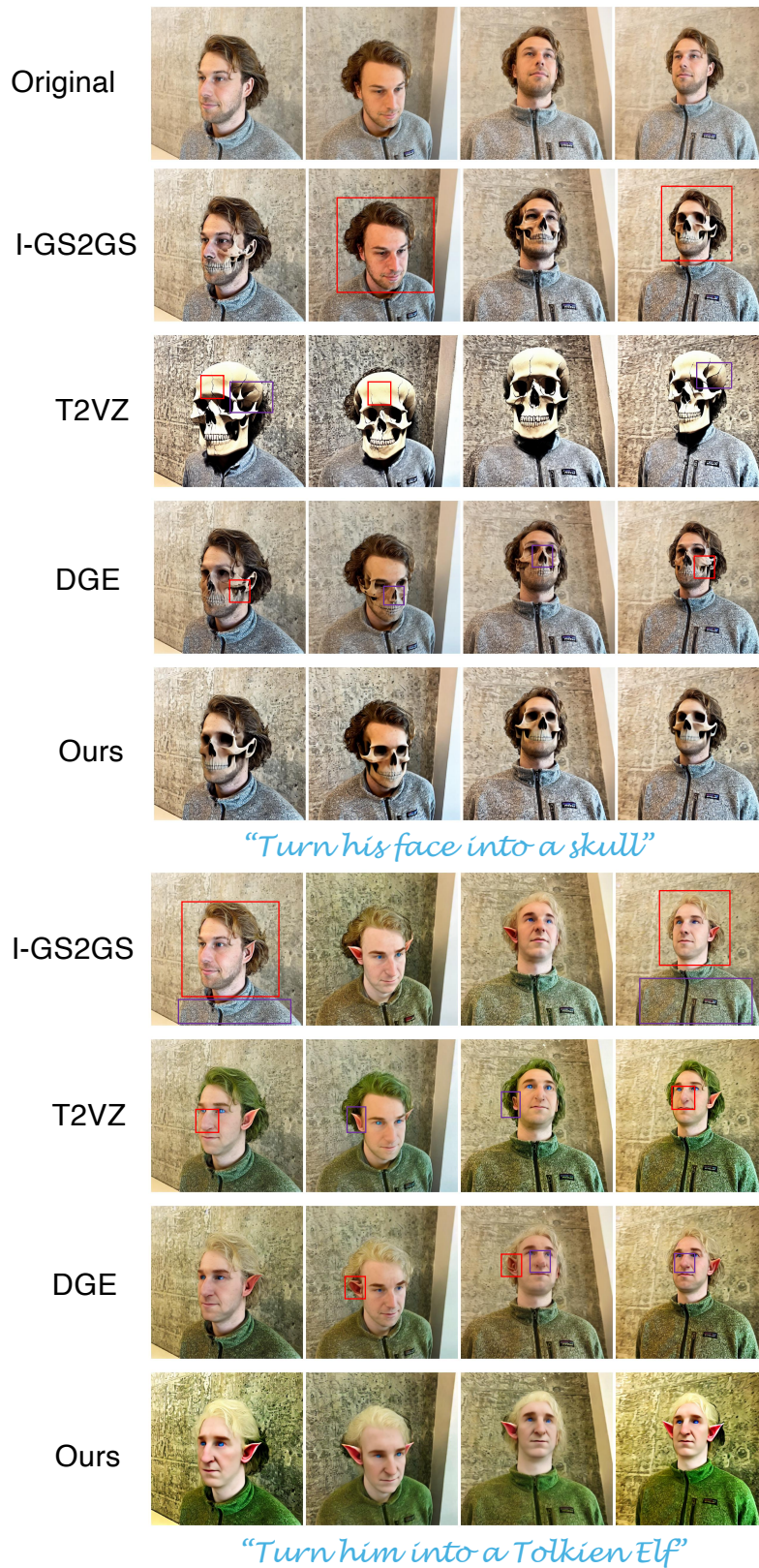


Figure 12. Comparison to baselines on Face scene edits.

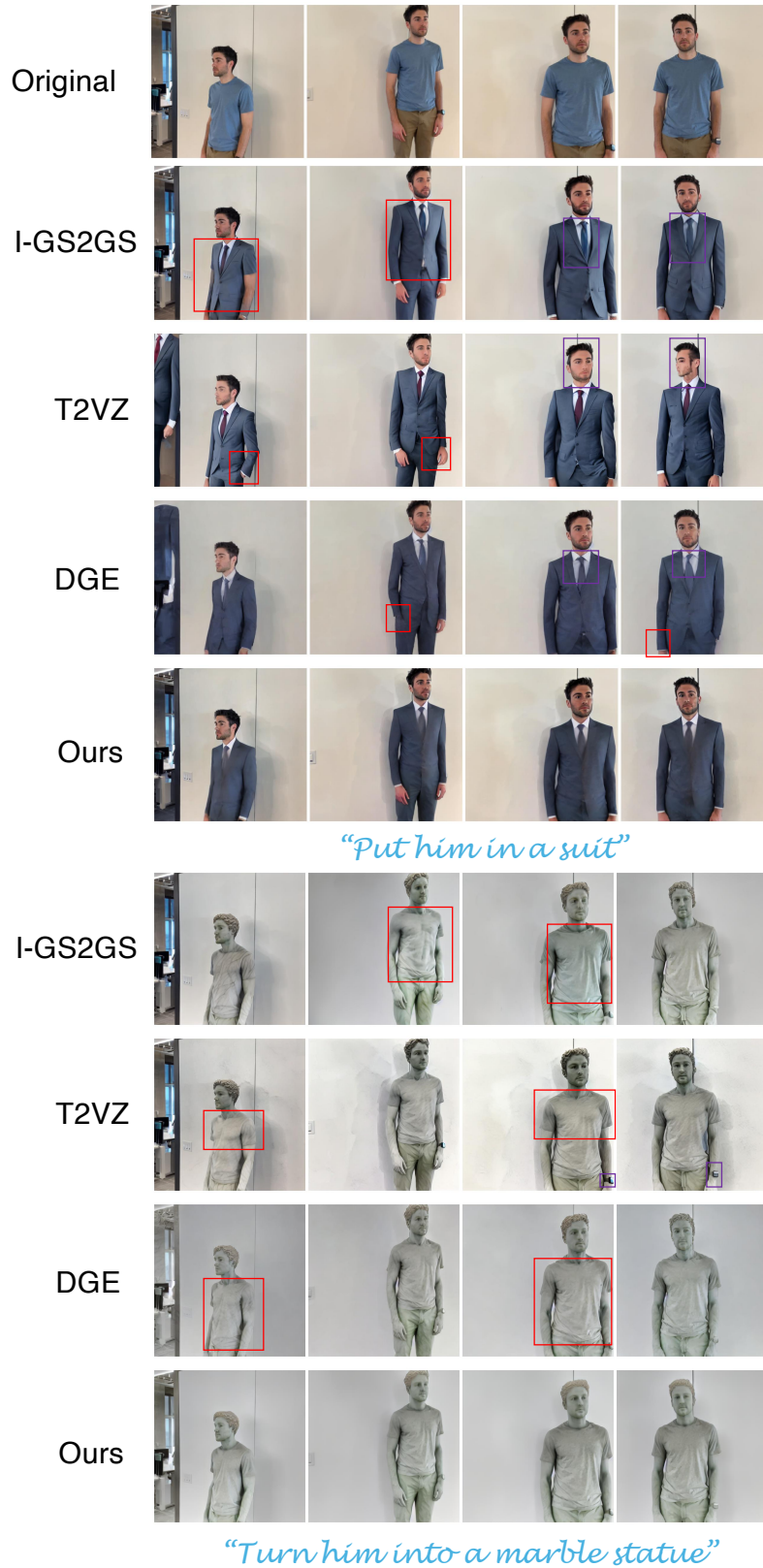


Figure 13. Comparison to baselines on Person scene edits.

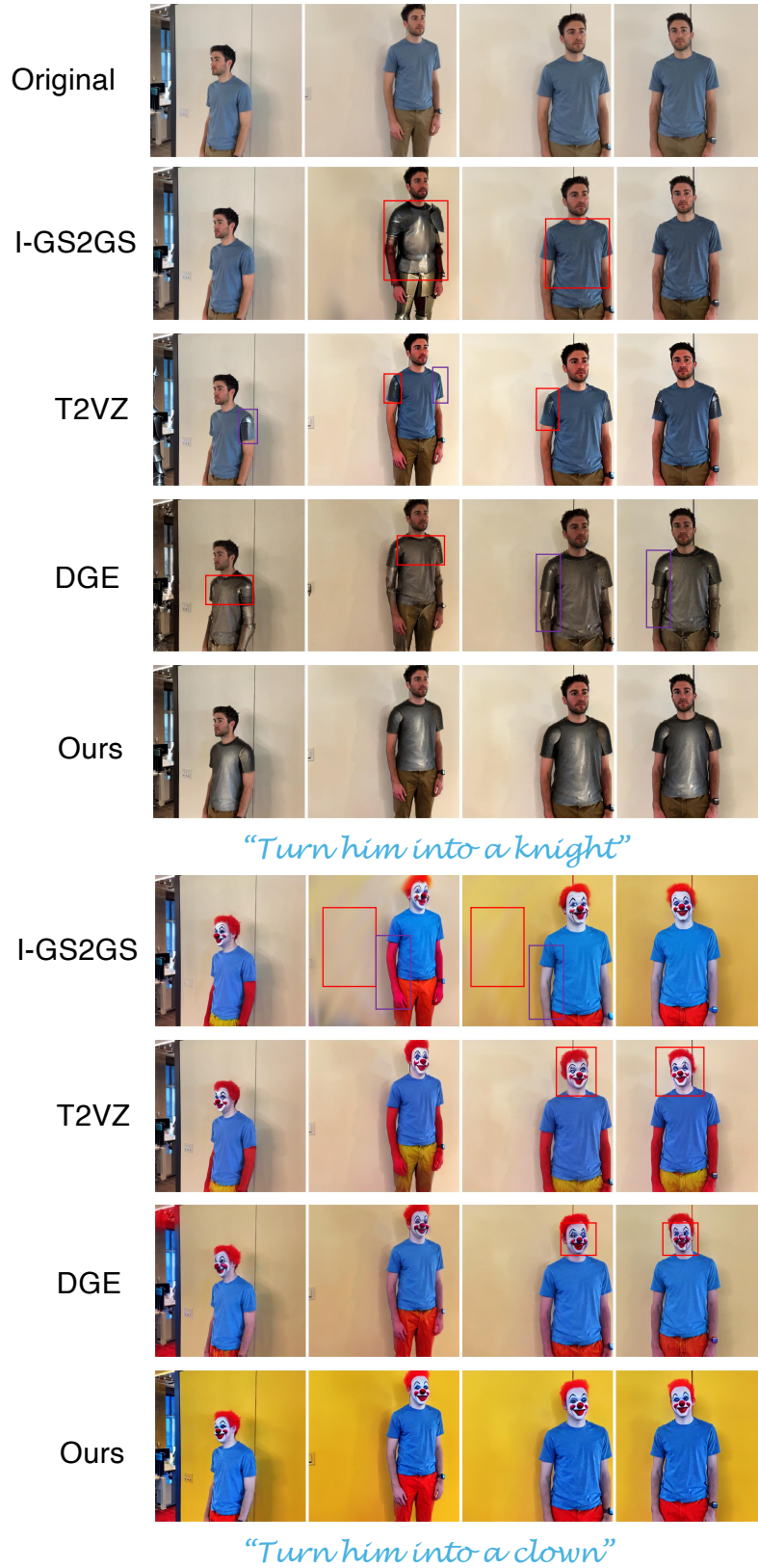
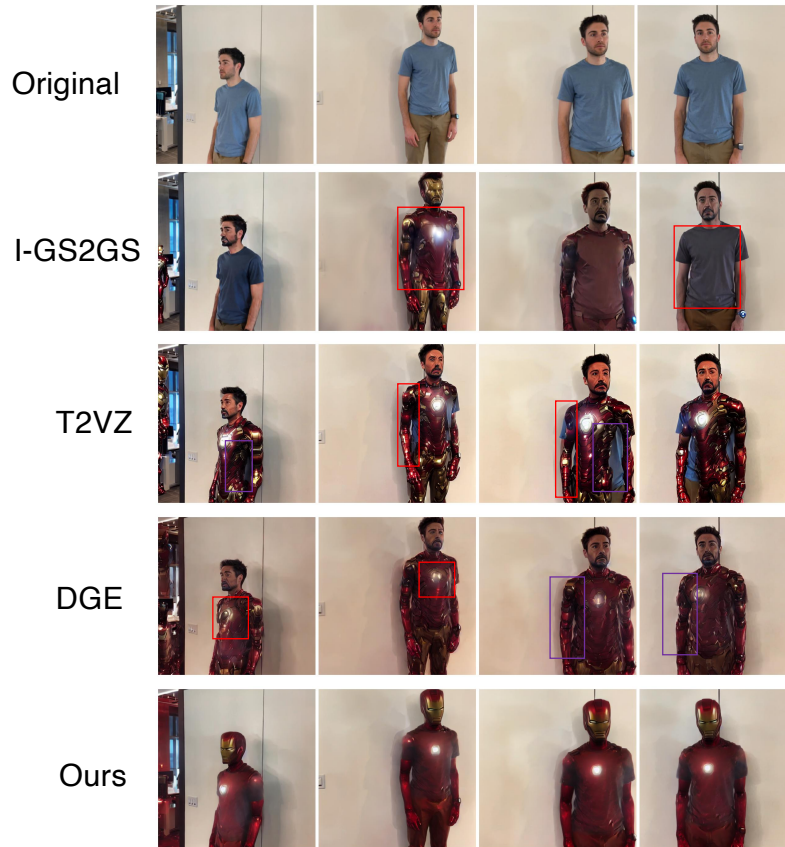
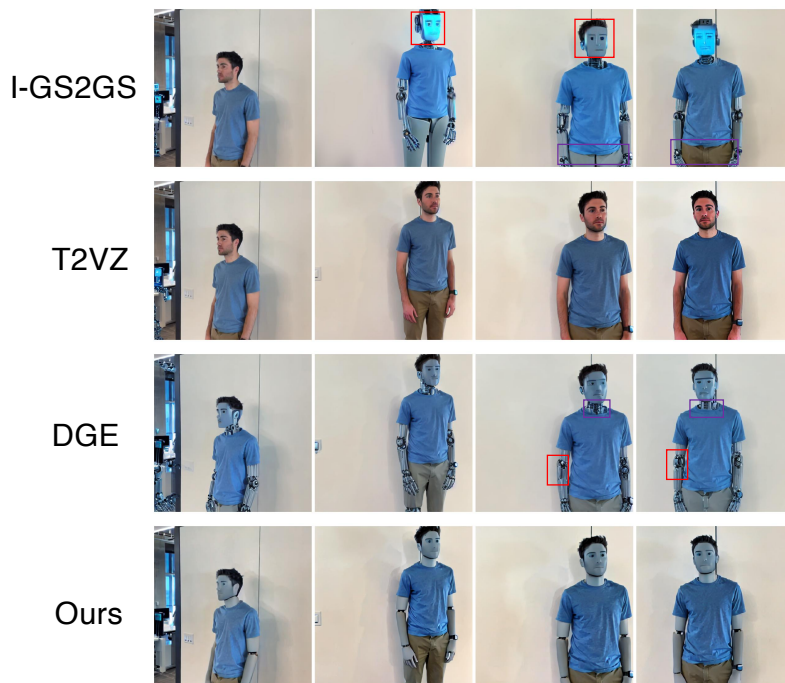


Figure 14. Comparison to baselines on Person scene edits.

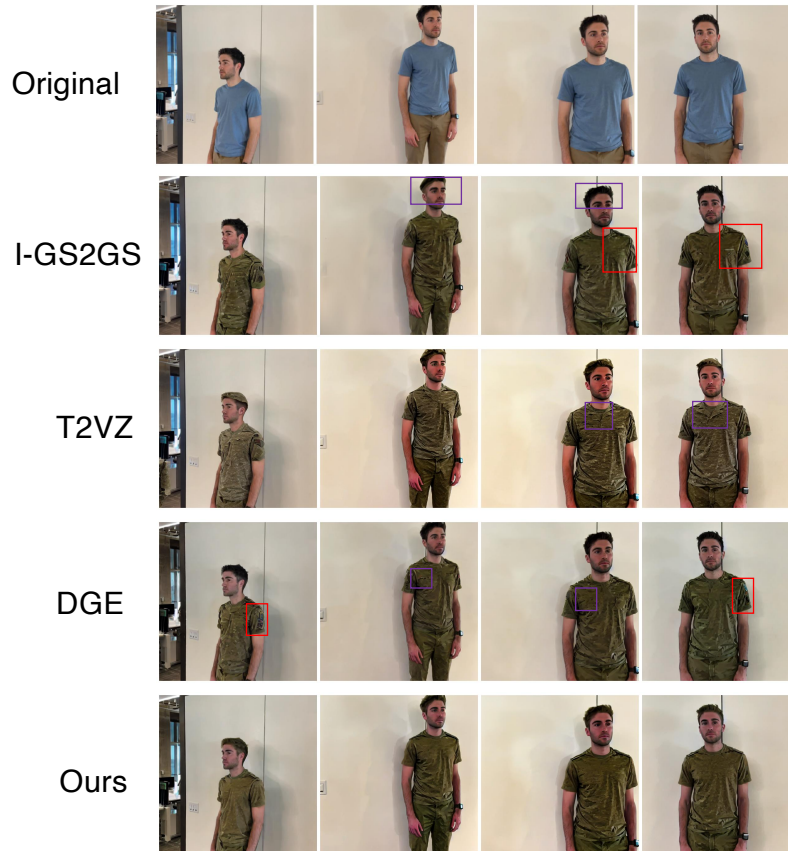


“Turn him into Iron Man”



“Turn him into a robot”

Figure 15. Comparison to baselines on Person scene edits.



“Turn him into a soldier”



“Turn him into a cowboy with a hat”

Figure 16. Comparison to baselines on Person scene edits.

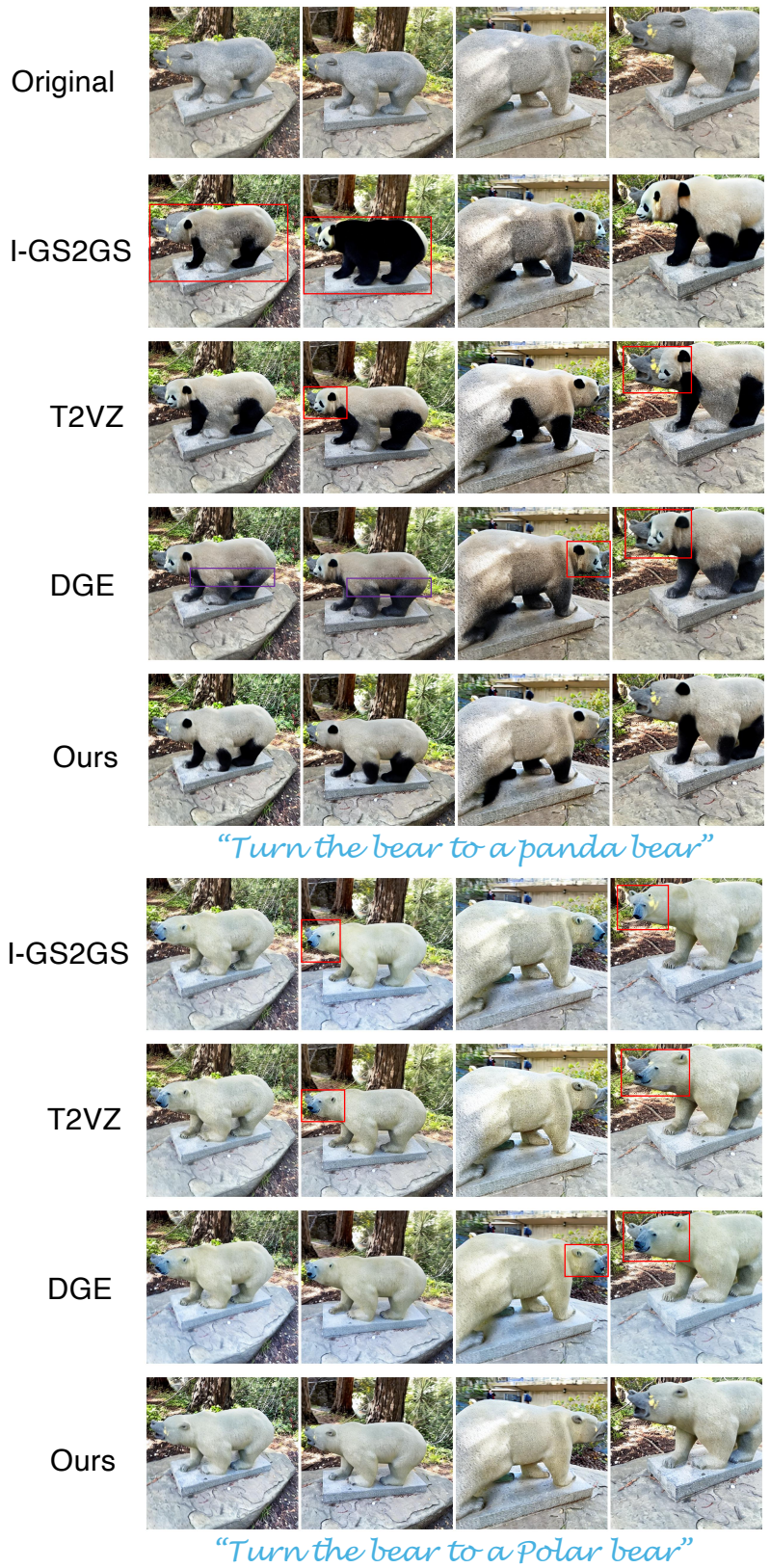
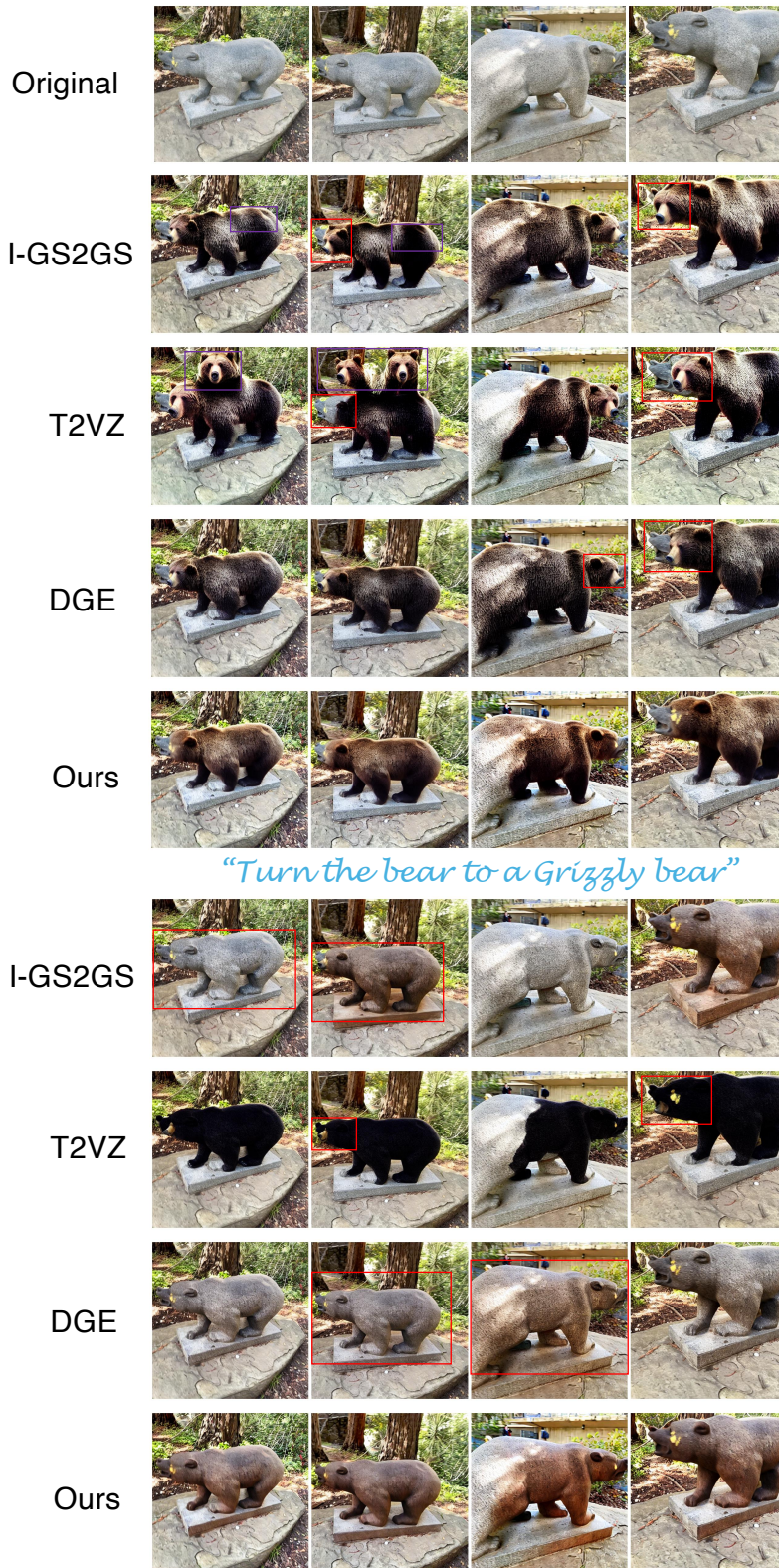


Figure 17. Comparison to baselines on Bear scene edits.



“Turn the bear to a wooden bear”

Figure 18. Comparison to baselines on Bear scene edits.



Original



"Make it night"



"Make it snowy"



Original



"Swap the plant with roses"



"Make the table out of rosewood"

Figure 19. I-Mix2Mix edits on the Car (top three rows) and Garden (bottom rows) scenes.



Original



"Make it during sunset"



"Change the statue to gold"



Original



"Make it spring"



"Make the floor out of ice"

Figure 20. I-Mix2Mix edits on the Horse (top three rows) and Ignatius (bottom rows) scenes.



Original



"Give him face paint"



"Turn him into Albert Einstein"



Original



"Turn him into a Polar bear"



"Turn him into a Grizzly bear"

Figure 21. I-Mix2Mix edits on 8 input frames on Face and Bear scenes.

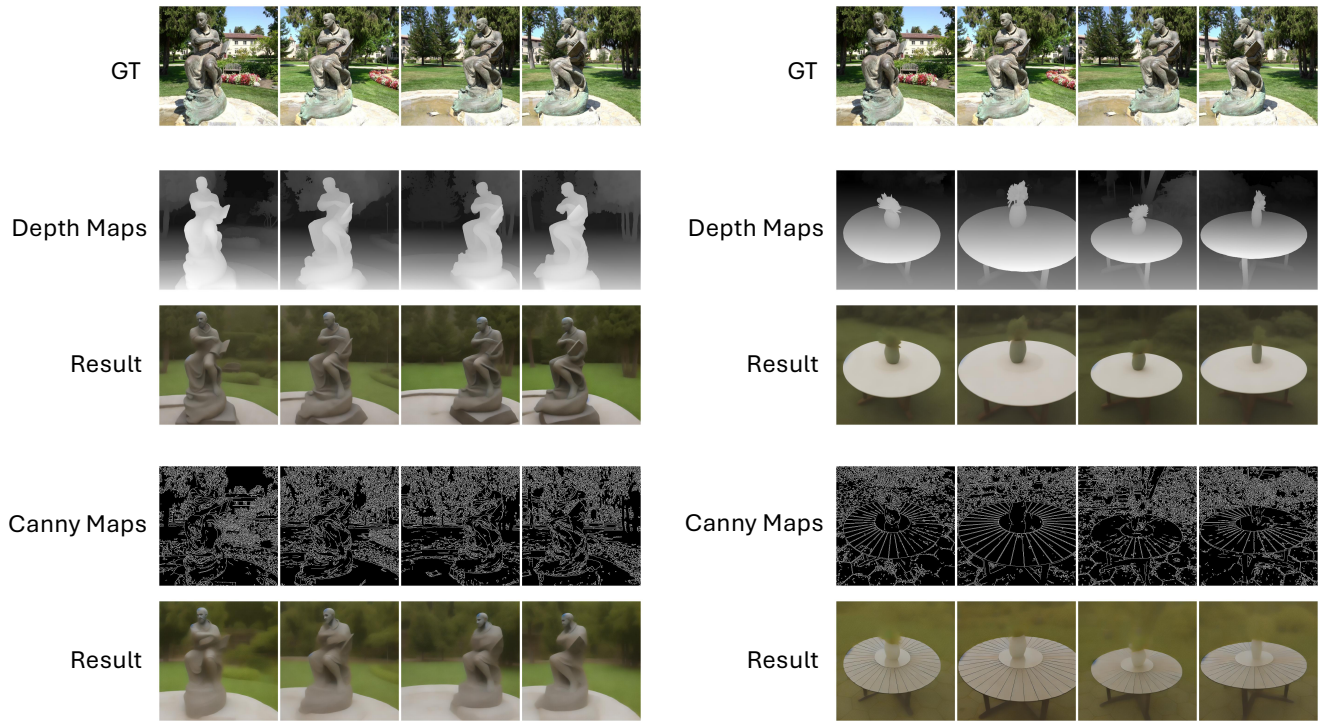


Figure 22. Example results of I-Mix2Mix with Canny edge map and Depth maps as input, with corresponding ControlNet teachers.

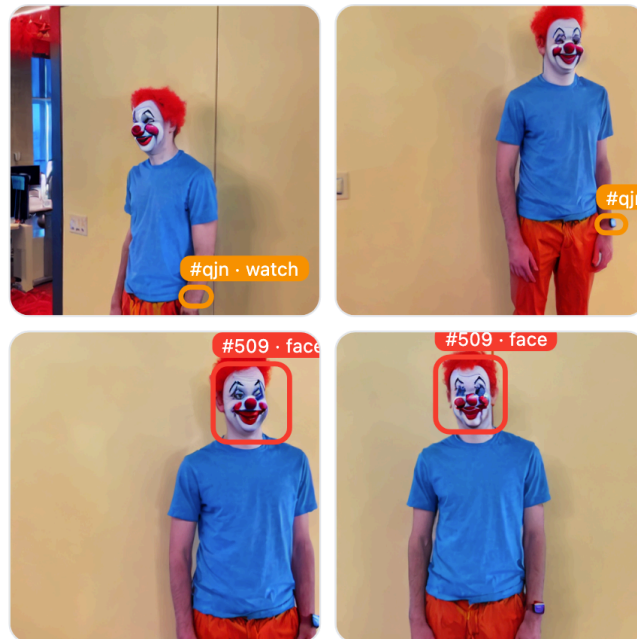


Figure 23. Example of inconsistencies in a scene marked by a human rater.